

# **Towards a consistent model for prediction of zeta potential in silica microchannels with respect to electrolyte properties in thermal equilibrium**

A Thesis  
Presented to the Faculty of the Graduate School  
of Cornell University  
in Partial Fulfilment of the Requirements for the Degree of Master of Science

by  
Vahnood Pourahmad  
May 2012

©2012 Vahnood Pourahmad

## ABSTRACT

Electroosmosis flow refers to motion of liquids induced by an applied voltage across microchannels.<sup>1</sup> This phenomenon has been known for a couple of centuries now and since then it has been used in a variety of technological applications (inkjet printer technology, electrochromatography, isoelectric focusing, etc. [1–3] and is still drawing even more attention from the scientific community particularly because of its relevance to micro-scale technology.

Electroosmosis is known to be first formulated in its present form by von Smoluchowski. [4]. He predicted that bulk fluid velocity under application of an external electric field would be equal to:

$$U_b = -\frac{\epsilon E_{ext}}{\eta} \zeta \quad (0.1)$$

where  $E_{ext}$  shows the external electric field applied tangentially to microchannel surface and  $\eta$  and  $\epsilon$  refer to fluid bulk viscosity and electrical permittivity respectively.

The  $\zeta$  term was then introduced to represent the scalar electric potential at the so called "shear plane" where the no-slip boundary condition applies. Smoluchowski's formula(2.4) is the most famous, fundamental equation in microfluidics and is used extensively in both research and design applications. Nevertheless and like many other physical formulae, it has been derived by making a few simplifying assumptions that are not necessarily always true.

---

<sup>1</sup> [en.wikipedia.org/wiki/Electro-osmosis](http://en.wikipedia.org/wiki/Electro-osmosis)

In One of the early modifications to(2.4), Overbeek and Lyklema [5], modified the formula and accounted for variability of  $\eta$  and  $\epsilon$  inside the so called "double layer" based on previous evidence from the theory of double layer capacitance in electrochemistry and experiments on the effects of electric field on viscosity of fluids [6, 7].

Recently researchers have studied interesting nonlinear AC electrokinetic phenomenon and come up with new intriguing experiments [8–11]. The novel results of these experiments have once again led researchers to consider modifying the classical equations of electrokinetics in order to explain their experimental observations. [11]

Yet another reason to urge for doing more research on the Helmholtz-Smoluchowski classic electokinetic theory comes from undesirable discrepancy between different data sets on  $\zeta$  potential measurements of certain solid-liquid interfaces. Notably Kirby and Hasselbrink, pointed out this problem in their 2004 paper and proposed normalization of measured  $\zeta$  potential by ionic strength of solutions which resulted in a better agreement between the various data sets [12].

The goal of this project which started on May 2009 under professor B.J Kirby's supervision was then to look for a way to either modify the classical electokinetic phenomenon theory or provide interpretation of available data sets on  $\zeta$  potential measurements in the literature such that this discrepancy can be explained. This would result in a better understanding and insight to the physics of double layer theory and fluid mechanics and better models to rely on in engineering design applications where prediction and control of zeta potential in microchannels is crucial.

## BIOGRAPHICAL SKETCH

Vahnood Pourahmad received his bachelor of science from Sharif university of technology in Tehran, Iran from the department of Civil & Environmental Engineering in 2008. He then got admitted to the M.S/Ph.D program in the field of Theoretical and Applied Mechanics at Cornell university where he is currently working towards getting his master of science degree.

## Acknowledgments

I am in great debt to professor T.J.Healey for his kind supports throughout this project and my advisor professor Brian Kirby for sharing his time and deep knowledge in fluid mechanics with me.

## CONTENTS

1. <i>Modeling the electrochemistry of the double layer</i> . . . . .	1
2. <i>Fluid mechanics of the double layer theory</i> . . . . .	14
2.1 Classical view . . . . .	14
2.2 New models . . . . .	17
2.2.1 Viscoelectric effect . . . . .	17
2.2.2 Charge-induced thickening . . . . .	24
2.2.3 A reformulation of electrokinetic flow by Bingham- type fluid mechanics analysis . . . . .	28
3. <i>Experimental investigation of electroosmosis</i> . . . . .	35
3.1 Streaming potential, a more accurate formulation . . . . .	35
3.2 Current monitoring measurement of <i>zeta</i> in Silica micro-capillaries	42
3.2.1 A new data set for Silica micro-capillary for alkaline buffers . . . . .	42
3.2.2 A proposed $\zeta$ potential measurement method based on excess electrostatic pressure in the double layer . .	55
4. <i>Conclusion</i> . . . . .	58

## 1. MODELING THE ELECTROCHEMISTRY OF THE DOUBLE LAYER

In the introduction chapter, electroosmosis and some relevant parameters were briefly introduced. It is very well known [12] that the  $\zeta$  term in Smoluchowski's equation is generally a function of the physical properties of both solid and liquid phases that are in contact with each other. In this chapter first a more vivid picture of the phenomenon will be presented and it will be followed by derivation of a detailed electrochemical model that is used through the rest of this work for prediction of  $\zeta$  potential of Silica based microchannels.

Electroosmosis becomes possible as a result of electric charge formation at the solid-liquid interface which in turn produce a net charge density profile in the double layer that extends from the interface up to several nanometers into the fluid phase. When an external electric field is applied tangentially to the channel surface, the net electrostatic force exerted on the charged double layer moves the layer, the rest of fluid will then be moved by means of viscous forces present in the fluid.[Fig.1.1]

The origins of the surface charge are different from one type of solid-liquid interface to another. For silica based surfaces the generally accepted hypothesis is that it is due to a chemical reaction in which water acts as a weak base and deprotonates silanol groups at the surface leaving them negatively charged. However for hydrophobic materials (Zeonor, polymers, etc) the surface charge origins is under dispute and different explanations have been proposed by different researchers, including hydroxyl ions specific adsorption, preferential orientation of water molecules at the hydrophobic surfaces, etc, [13] yet none of these theories has been generally agreed upon.

For our modeling purposes, we assume that a layer of Silanol groups furnishes the surface of a glass/silica/quartz capillary, and we represent the local site density of these groups by  $n_s$ . A Silanol group has an  $SiOH$  branch which furnishes the surface and as mentioned earlier when these groups lose



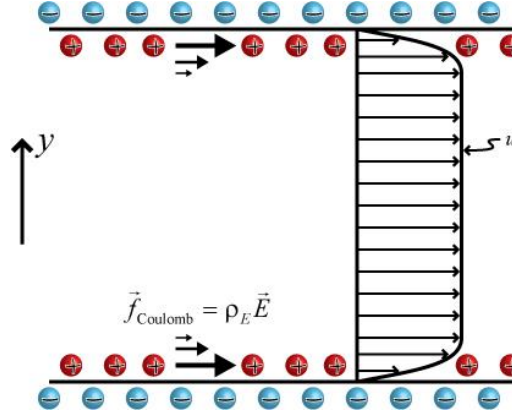


Fig. 1.1: Electroosmosis phenomenon, courtesy of B.Kirby

one  $H^+$  ion, a layer of  $SiO^-$  groups remains at the surface which gives the surface its negative charge and its associated electric potential.[Fig.1.2]

With this picture in mind it is obvious that interfacial potential,  $\varphi_o$ , should be a strong function of pH of solution and that an increase in pH should result in increase in the magnitude of  $\varphi_o$  since then more and more  $SiOH$  groups are willing to lose their protons. This general trend has indeed been observed and verified in experiments [12, 14, 15].

As illustrated in figure(1.2), dissolved metal cations (shown by M circles in the figure) may also get adsorbed to the surface and react with the left  $SiO^-$  groups and thus cancel out some of the negative charge produced at the surface. Hence it seems that the interfacial potential should also be a function of cation concentration or equivalently concentration of dissolved salt in the liquid phase. In this section the concentration of dissolved salt in molar is represented by  $C_s$  and the minus of its logarithm by  $pC_s = -\log_{10}(C_s)$ . Since presence of more dissolved cations at the surface results in cancelation of more left negative charges at the surface, one expects a decrease in the magnitude of  $\varphi_o$  when  $C_s$  increases as another general trend.

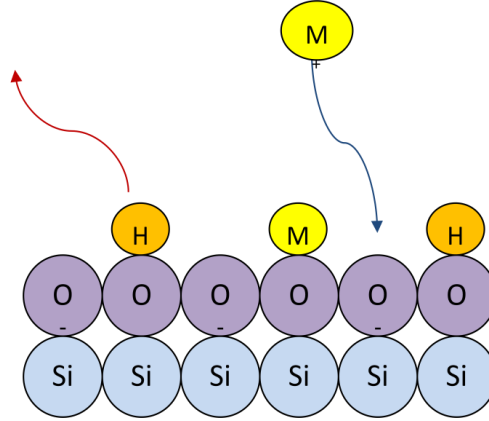
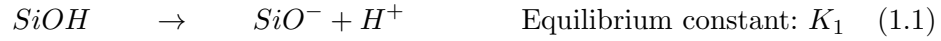
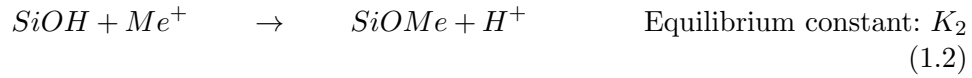


Fig. 1.2: The chemical reactions at the silica water interface

To complete the list of chemical parameters needed, we need to define two more parameters which are the equilibrium rate constants for the two main reactions that are assumed to occur at the interface, the first one is that of deprotonation of Silanol groups:



and the second is that of metal cation reaction with the Silanol groups:



It follows then that at equilibrium, the following set of equations should be satisfied:

$$[SiOH] + [SiO^-] + [SiOMe] = n_s \quad (1.3)$$

$$\frac{[SiO^-][[H^+]]}{[SiOH]} = K_1 \quad (1.4)$$

$$\frac{[SiOMe][[H^+]]}{[SiOH][[Me^+]]} = K_2 \quad (1.5)$$

where  $[ \cdot ]$  refers to site density of a species in sites per meters squared and  $[[ \cdot ]]$  refers to activity of a species which is the product of its activity coefficient and its local concentration in molar i.e :

$$[[ i ]] = \alpha_i \cdot [ i ]$$

where  $\alpha_i$  is called the "activity coefficient" of species "i" and  $[ i ]$  shows concentration of species "i" in molar.

We have thus been careful to use activities instead of species concentration of cations in above equations. It is possible that near a negatively charged surface, concentration of cations get high enough such that the "dilute solution" assumption breaks down. In this case using concentration of species instead of their activities in equilibrium equations leads to incorrect final answers. This indeed is very well known in Chemistry and in fact there are published data in chemistry handbooks [16] which give activity coefficients versus concentrations of species.

The discrete published data in the handbooks are not particularly useful for our purposes which requires implementing activity coefficients in a continuous quantitative model. We should instead come up with a continuous function that gives activity coefficients as a function of concentration.

For this reason, a Debye-Huckel type equation [?] for determining activity coefficient has been used and the constant coefficient in that equation were optimized such that an excellent fit to the published tables in [16] for

$H^+$  and  $K^+$  ions was obtained.

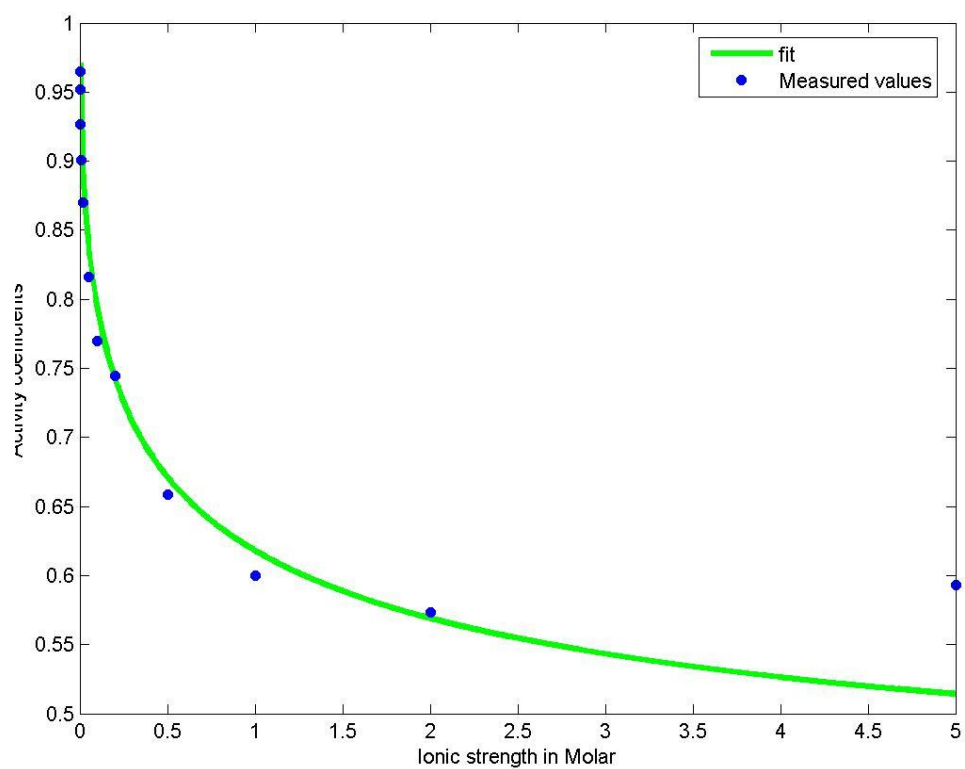
More precisely, the Debye-Huckel equation suggests that activity coefficient  $\alpha_i$  of species "i" is given as:

$$\alpha_i = \exp\left(\frac{-Az\sqrt{I}}{1 + Ba\sqrt{I}}\right) \quad (1.6)$$

where  $A$  and  $B$  are constant coefficients,  $I$  is the ionic strength of the solution,  $z$  is the valence and  $a$  is the effective diameter of the ion.

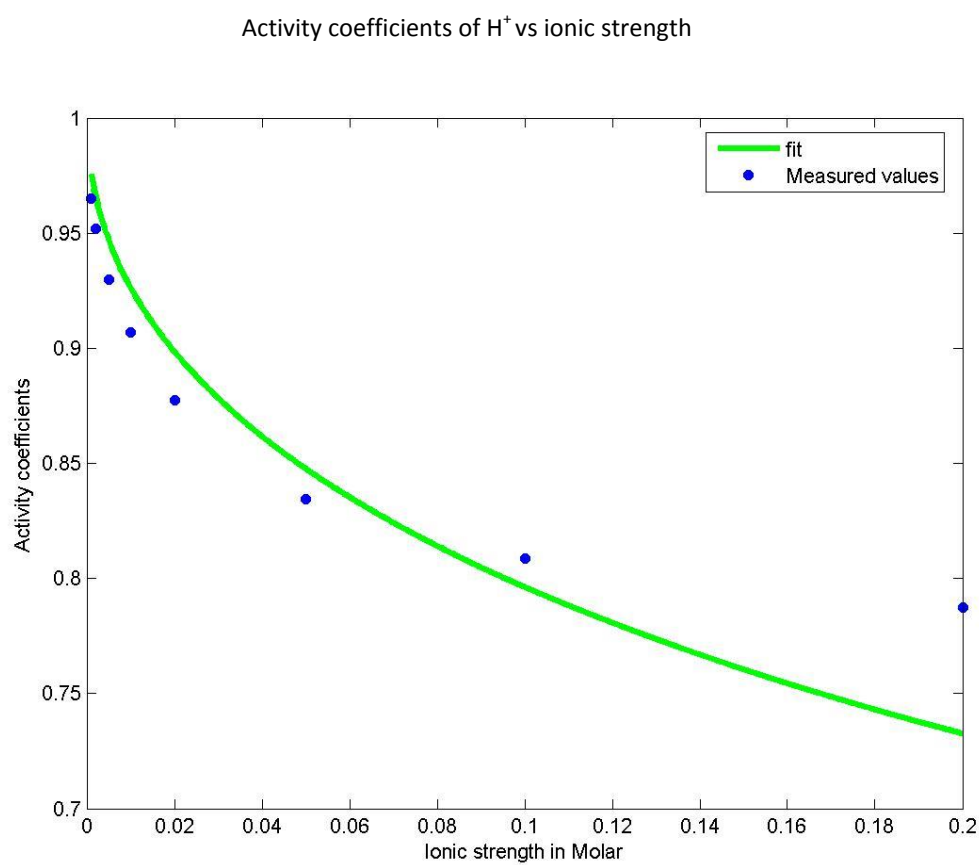
As mentioned earlier, by running an optimization process for determining constant coefficients in the above equation, an excellent fit for use in our MATLAB code for determining zeta potential has been achieved. Figures (1.3) and (1.4) show comparison of the predicted versus published values in [16] for activity coefficients for  $K^+$  and  $H^+$  ions respectively.

Activity coefficients of potassium ion vs ionic strength



$$\alpha = \exp\left(\frac{-0.9625\sqrt{I}}{1 + \sqrt{I}}\right)$$

Fig. 1.3: Activity coefficient of  $K^+$  ions



$$\alpha = \exp\left(\frac{-.7892\sqrt{I}}{1 + .3\sqrt{I}}\right)$$

Fig. 1.4: Activity coefficient of  $H^+$  ions

Once that activity coefficients are known we can define:

$$k_1 = \frac{K_1}{\alpha_{H^+}}$$

and

$$k_2 = \frac{K_2}{\alpha_{Me^+}}$$

and rewrite equations(1.4) and(1.5) as:

$$\frac{[SiO^-] [H^+]}{[SiOH]} = k_1$$

and

$$\frac{[SiOMe] [H^+]}{[SiOH] [Me^+]} = k_2$$

It should be noted however that since equation(1.6) needs concentration of species in order to calculate their activity coefficients, an iterative process is necessary for finding the concentration of species. We thus start by making a guess on  $\alpha_i$  values, concentrations of the species are then calculated from (1.4)and(1.5). The calculated concentrations are then plugged back into (1.6) to recalculate  $\alpha_i$  values. This iterative process continues until convergence occurs which would give the correct concentrations and activity coefficients.

According to Boltzmann distribution law, concentration of species "i" at the surface is related to its bulk concentration by:

$$C_i = C_b \exp \left( -\frac{Fz\varphi_o}{RT} \right)$$

If now we write local concentrations at the surface in terms of bulk concentration of species, we finally get the following three simultaneous equations at equilibrium:

$$[SiOH] + [SiO^-] + [SiOMe] = n_s \quad (1.7)$$

$$\frac{[SiO^-][H^+]_b}{[SiOH]} = k_1 \exp\left(\frac{F\varphi_o}{RT}\right) \quad (1.8)$$

$$\frac{[SiOMe][H^+]_b}{[SiOH][Me^+]_b} = k_2 \quad (1.9)$$

By solving the the above system of equations, we find the local density of  $SiO^-$  to be :

$$[SiO^-] = \frac{n_s k_1}{k_1 + ([H^+]_b + [Me^+]_b k_2) \exp\left(-\frac{F\varphi_o}{RT}\right)}$$

$\Rightarrow$

$$Q_o'' = \frac{-en_s k_1}{k_1 + ([H^+]_b + [Me^+]_b k_2) \exp\left(-\frac{F\varphi_o}{RT}\right)} \quad (1.10)$$

where  $e$  is the elementary charge constant and  $Q_o''$  shows charge density( i.e charge per unit area) at the wall. This equation is one way of determining charge density at the wall. There is yet another way of finding the surface charge density by applying the electro-neutrality condition for the



whole system in the following manner:

Right above the wall surface there exists a fluid medium in which different ions are floating around. Up to a certain point in this medium there exists net nonzero charge density and this particular part of the solution is generally called the "diffusive layer". The reason why there should be net charge density becomes evident if one considers the fact that since the surface wall is negatively charged, local concentration of cations are greater than those of anions so that a net positive charge should exist near the wall. This net charge density of course decays to zero in the bulk of fluid, moreover this net positive charge density screens the negative charge at the surface and electro-neutrality requires that the two should exactly balance out.

Mathematically speaking, from Boltzmann distribution law we have that local concentration of species "i" is:

$$C_i = C_{i,b} \exp\left(-\frac{Fz_i\varphi}{RT}\right) \quad (1.11)$$

so that net charge density at a particular point is:

$$\rho_e = \sum_i C_{i,b} F z_i \exp\left(\frac{-Fz_i\varphi}{RT}\right) \quad (1.12)$$

here summation is over all present species in the solution.

Upon application of Poisson's law ( $\rho_e = -\epsilon \frac{\partial^2 \varphi}{\partial y^2}$ ), equation(1.12) becomes:

$$\frac{\partial^2 \varphi}{\partial y^2} = \sum_i \frac{-C_{i,b} F z_i}{\epsilon} \exp\left(\frac{-Fz_i\varphi}{RT}\right)$$

or equivalently by multiplying both sides by  $\frac{\partial \varphi}{\partial y}$  :

$$\frac{\partial \varphi}{\partial y} \frac{\partial^2 \varphi}{\partial y^2} = \sum_i \frac{-C_{i,b} F z_i}{\epsilon} \exp\left(\frac{-F z_i \varphi}{RT}\right) \frac{\partial \varphi}{\partial y}$$

The integration of this last equation yields:

$$\left(\frac{\partial \varphi}{\partial y}\right)^2 \Big|_o^\infty = \sum_i \frac{2C_{i,b} RT}{\epsilon} \exp\left(\frac{-F z_i \varphi}{RT}\right) \Big|_o^\infty$$

by realizing that  $\frac{\partial \varphi}{\partial y} = E \rightarrow 0$  and  $\varphi \rightarrow 0$  as  $y \rightarrow \infty$

we get the so called Grahmme's equation for finding the magnitude of electric field at the surface  $E_o$  :

$$|E_o| = \sqrt{\sum_i \frac{2C_{i,b} RT}{\epsilon} \exp\left(\frac{-F z_i \varphi_o}{RT}\right)} \quad (1.13)$$

It is worth to note that in deriving Grahmme's equation, absolutely no numerical approximation is made and as long as Boltzmann distribution law is valid, this equation is exactly true. The importance of Grahmme's equation in the current context is that it enables us to get a relation for the charge density in the diffuse layer.

As illustrated in figure(1.5), if we draw a sufficiently large control volume that encloses the whole diffuse layer then the charge enclosed in the control volume is equal the total net charge in the diffuse layer. Then according to Gauss's law in electrodynamics we know:

$$Q_{enc} = \int_V \rho_e dv = \int_S \epsilon \mathbf{E} \cdot d\mathbf{s} \quad (1.14)$$

The surface integral in the above equation is easy to evaluate:(see [Fig.1.5])

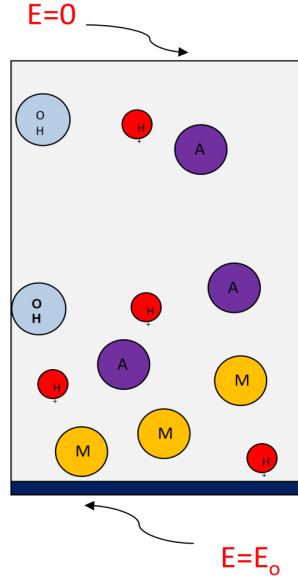


Fig. 1.5: A control volume around diffuse layer

$$Q''_{enc} = -\epsilon E_o = \epsilon |E_o|$$

Since  $E_o < 0$  for a negatively charged surface.

Finally using Grahmme's equation to find  $|E_o|$  we get:

$$Q''_{enc} = \sqrt{\sum_i 2\epsilon C_{i,b} RT \exp\left(\frac{-F z_i \varphi_o}{RT}\right)} \quad (1.15)$$

and electro-neutrality of the system requires that  $Q''_o + Q''_{enc} = 0 \Rightarrow$

$$\frac{-en_s k_1}{k_1 + ([H^+]_b + [Me^+]_b k_2) \exp\left(-\frac{F\varphi_o}{RT}\right)} + \sqrt{\sum_i 2\epsilon C_{i,b} RT \exp\left(\frac{-F z_i \varphi_o}{RT}\right)} = 0 \quad (1.16)$$

Equation(1.16)is the main equation that will be used in the rest of this work in order to predict interfacial potential, $\varphi_o$ ,as a function of pH and salt concentration. Comparison between model prediction and the experimental data is presented in the concluding chapter.

## 2. FLUID MECHANICS OF THE DOUBLE LAYER THEORY

### *2.1 Classical view*

As pointed out in the introduction, Smoluchowski originally formulated electroosmosis theory and derived a basic formula for a fluid's bulk electrokinetic velocity. In this section this basic formula is derived so that it can be compared with the more complex formulations that will be presented in the later sections.

We start by Navier-Stokes equations in low Reynolds number regime:

$$-\nabla P + \eta \nabla^2 \mathbf{v} + \mathbf{B} = 0 \quad (2.1)$$

What makes electokinetic fluid dynamics different from conventional fluid mechanics problems, lies in the body force term  $\mathbf{B}$ . This term arises because of the presence of net electric charge in the double layer which upon application of an external, tangential electric field exerts a net electrostatic force on the fluid.

This body force term is simply equal to:

$$\mathbf{B} = \rho_e \mathbf{E}_{ext}$$

Upon application of Poisson's law in electrodynamics, we get:

$$\mathbf{B} = -\epsilon \nabla^2 \varphi \cdot \mathbf{E}_{ext} \quad (2.2)$$

Where  $\varphi$  is defined as the electric potential difference at any point with respect to the bulk electric potential, now by assuming that no pressure gradient is applied along the channel we get:

$$\nabla^2 \mathbf{v} = \frac{\epsilon \mathbf{E}_{ext}}{\eta} \nabla^2 \varphi$$

Further if we assume that radius of curvature of the capillary is much larger than double layer thickness then we can use 1-D formulation of the above equation to get:

$$\frac{\partial^2 v}{\partial y^2} = \frac{\epsilon E_{ext}}{\eta} \frac{\partial^2 \varphi}{\partial y^2}$$

We integrate this equation two times and upon applying the appropriate boundary conditions:

$$y = 0 : \quad \varphi = \varphi_o \quad \text{and} \quad v = 0$$

$$y \rightarrow \infty : \quad \varphi = 0 \quad \text{and} \quad v = U_b$$

we get:

$$U_b = -\frac{\epsilon E_{ext}}{\eta} \varphi_o \tag{2.3}$$

This is the so called Smoluchowski's equation which gives the bulk electroosmotic fluid velocity in terms of electric potential at the interface (interfacial potential  $\varphi_o$ ) and other relevant parameters involved. The electric potential at the interface, or more precisely at the shear plane, has been given a special name and traditionally is called "zeta" ( $\zeta$ ) potential and thus Smoluchowski's relation is usually written as:

$$U_b = -\frac{\epsilon E_{ext}}{\eta} \zeta \tag{2.4}$$

where  $\zeta = \varphi_o$

## 2.2 *New models*

### 2.2.1 *Viscoelectric effect*



Lyklema and Overbeek first introduced the concept of viscoelectricity [5] and predicted saturation of electroosmotic mobility with increasing interfacial potential. In this section, first I propose a different physical explanation that came to my mind for the viscoelectric dependence of fluid viscosity to the intrinsic electric field. I then derive the formula that Lyklema and Overbeek got for the bulk fluid mobility. This will be used for later comparison of different proposed fluid mechanics theories of the double layer.

It came to my mind that if the viscosity of water increases at higher densities, then electroosmotic mobility may saturate at higher interfacial potentials due to possible increase in the density of highly polarizable water molecules. In trying to formulate this idea I got the exactly same functional dependence as the one proposed by Lyklema and Overbeek for viscoelectric effect. In what follows a linear relationship is assumed between density and viscosity of water and a quadratic relation is then found between viscosity of fluid and intrinsic normal electric field in the double layer.

According to Boltzmann distribution law, concentration of species is an exponential function of their potential energy normalized by thermal energy of particles :

$$C = C_b \exp \left( -\frac{E_i}{KT} \right) \quad (2.5)$$

where  $E_i$  shows the energy of particles in the  $i$ th state.

A nonuniform potential energy field results in a nonuniform concentration profile in space, this in fact is the basis of Poisson-Boltzmann equation for determining the concentration profile of charged species in double layer and hence is the core of the so called Gouy-Chapmann theory of double layer which is discussed in detail elsewhere[17–20].

In the case of charged particles, there is an obvious associated electric potential energy with each particle  $E = q\varphi$  where  $\varphi$  is the electric potential field, however for uncharged particles like water molecules, at first, it seems that there is no stored electric potential energy because their net charge is zero, hence we do not expect nonuniformity in their concentration throughout the double layer although electric potential field is nonuniform.

Nevertheless this insight may change if we remember that water molecules are polarizable molecules and positive and negative poles get separated by some distance when experiencing an electric field. Thus in an exponentially decaying electric potential field, like the one in the double layer, due to extremely fast decay of the electric potential field, opposite poles experience different potentials which do not exactly cancel out each other and hence a water molecule can have a finite electric potential energy.

In order to formulate the above qualitative argument, we denote dipole moment of a water molecule by  $p = qa$  where  $q$  is the charge of each opposite pole and  $a$  being the distance by which the poles are separated then from fundamental Electrodynamics one knows that:

$$P = \epsilon_o \chi E \quad (2.6)$$

$$\begin{array}{ll} P : & \text{Average dipole moment} = \frac{\sum p}{V} \\ \epsilon_o : & \text{Vacuum electric permittivity} \\ \chi : & \text{Relative permittivity of the medium} \\ E : & \text{Electric field} \end{array}$$

If we show concentration of particles in millimolar by  $m$  and Avogadro's number by  $N_a$  then:

$$\begin{aligned} p &= \frac{\epsilon_o \chi E}{m N_a} \Rightarrow \\ q &= \frac{\epsilon_o \chi E}{m a N_a} \end{aligned} \quad (2.7)$$

In the case of negative interfacial potential where electric field is also negative then net associated electric potential is:

$$\begin{aligned}
V &= -q\varphi\left(\mathbf{r} + \frac{\mathbf{a}}{2}\right) + q\varphi\left(\mathbf{r} - \frac{\mathbf{a}}{2}\right) \Rightarrow \\
V &= -q\mathbf{a} \cdot \nabla\varphi(\mathbf{r})
\end{aligned} \tag{2.8}$$

By realizing that  $\nabla\varphi(\mathbf{r}) = -E(\mathbf{r})$  and taking care of the sign conventions we find that in general:

$$\begin{aligned}
V &= -\frac{\epsilon_o\chi E}{maN_a}aE \quad \Rightarrow \\
V &= -\frac{\epsilon_o\chi E^2}{mN_a}
\end{aligned} \tag{2.9}$$

so according to(2.5), density of water molecules at a particular location is :

$$C = C_b \exp\left(\frac{\epsilon_o\chi E^2}{mRT}\right) \tag{2.10}$$

Finally if we assume a linear relationship between viscosity and density of water molecules, i.e that :

$$\eta = \frac{C}{C_b}\eta_b$$

we get:

$$\eta = \eta_b \exp\left(\frac{\epsilon_o\chi E^2}{mRT}\right) \tag{2.11}$$

If we call  $\left(\frac{\epsilon_o \chi}{mRT}\right)$  ,  $f$  then://

$$\eta = \eta_b \exp(fE^2)$$

A simple calculation shows that for water at room temperature  $f \simeq 5.16 \cdot 10^{-18}$  so that for a typical value of  $E \simeq 10^7$  still the argument of the exponential function is pretty small (approximately .013 ), since:

$$\exp(s) \simeq 1 + s \quad s \ll 1$$

then we conclude:

$$\eta = \eta_b(1 + fE^2) \tag{2.12}$$

This equation looks exactly like the one Lyklema and Overbeek have phenomenologically proposed except for the difference in the calculated value of viscoelectric coefficient which turns out to be  $f = 5 \cdot 10^{-18}$  here which is different from the value of  $f = 10^{-14}$  that they proposed.

The importance of viscoelectric effect is in that it results in a new relationship between interfacial and zeta potentials which is different from the classical one derived by Smoluchowski and that it helps in reducing the over prediction of zeta potential based on electrochemical properties of solid-liquid interface.

To be more precise, as shown in [11], the bulk fluid velocity can be calculated as:

$$U_b = E_{ext} \int_{\varphi_o}^0 \frac{\epsilon}{\eta} d\varphi \tag{2.13}$$

In the Debye-Huckel limit we have:

$$\varphi = \varphi_o \exp\left(-\frac{y}{\lambda_D}\right) \Rightarrow E = -\frac{d\varphi}{dy} = \frac{1}{\lambda_D} \varphi_o \exp\left(-\frac{y}{\lambda_D}\right)$$

$\Rightarrow$

$$E = \frac{1}{\lambda_D} \varphi \quad (2.14)$$

using(2.14) in (2.12) and plugging them back into (2.16) results in:

$$U_b = \frac{\epsilon E_{ext}}{\eta_b} \int_{\varphi_o}^0 \frac{1}{1 + \frac{f}{\lambda_D^2} \varphi^2} d\varphi$$

$\Rightarrow$

$$U_b = \frac{\lambda_D \epsilon E_{ext}}{\eta_b \sqrt{f}} \arctan\left(\frac{\sqrt{f}}{\lambda_D} \varphi\right) \Big|_{\varphi_o}^0$$

$\Rightarrow$

$$U_b = -\frac{\lambda_D \epsilon E_{ext}}{\eta_b \sqrt{f}} \arctan\left(\frac{\sqrt{f}}{\lambda_D} \varphi_o\right)$$

so that the effective zeta potential in this case is:

$$\zeta_{eff} = \frac{U_b}{-\frac{\epsilon E_{ext}}{\eta_b}} = \frac{\lambda_D}{\sqrt{f}} \arctan\left(\frac{\sqrt{f}}{\lambda_D} \varphi_o\right) \quad (2.15)$$

2.2.2 *Charge-induced thickening*

Recently [11, 21] M.Bazant, though in a different context from this work, has hypothesized that the viscosity and electrical permittivity of a fluid is not uniform throughout the double layer and postulated the following equation for their variation with respect to counter-ion density in the double layer:

$$\frac{\epsilon}{\eta} = \frac{\epsilon_b}{\eta_b} \left( 1 - \frac{\rho}{\rho_m} \right) \quad (2.16)$$

Where  $\rho$  is the charge density at a given point and  $\rho_m$  refers to the hypothesized maximum charge density at which the viscosity of fluid goes to infinity and fluid flow stops.

In this section the same idea is applied to get an equation for effective zeta,  $\zeta$ , in terms of interfacial potential which turns out to be a quadratic relation between the two in the Debye-Huckel regime.

Bazant [11], has shown that the bulk fluid velocity can be calculated via:

$$U = E_{ext} \int_{\phi_o}^0 \frac{\epsilon}{\eta} d\phi \quad (2.17)$$

Now in a symmetric electrolyte solvent, if we assume Boltzmann distribution for the density of particles then:

$$\rho = -2eFC_b \sinh \left( \frac{Fz\phi}{RT} \right) \quad (2.18)$$

using this equation for the density of counter ions in equation (2.16) and plugging that back into (2.17) we get:

$$U_b = E_{ext} \frac{\epsilon_b}{\eta_b} \int_{\phi_o}^0 \left( 1 + \frac{2C_b}{C_m} \sinh \left( \frac{Fz\phi}{RT} \right) \right) d\phi$$



which is tantamount to:

$$U_b = \frac{\epsilon_b E_{ext}}{\eta_b} \left( -\varphi_o + \frac{2C_b RT}{FzC_m} \left( 1 - \cosh\left(\frac{Fz\varphi_o}{RT}\right) \right) \right) \quad (2.19)$$

we can further simplify the above equation by noting that:

$$1 - \cosh(s) = -2 \sinh^2\left(\frac{s}{2}\right)$$

thus (2.19) is equivalent to:

$$U_b = \frac{\epsilon_b E_{ext}}{\eta_b} \left( -\varphi_o - 4 \frac{C_b RT}{FzC_m} \sinh^2\left(\frac{Fz\varphi_o}{2RT}\right) \right) \quad (2.20)$$

Finally we define  $\zeta_{eff}$  as:

$$\zeta_{eff} = -\frac{\eta_b}{\epsilon_b E_{ext}} U_b \quad (2.21)$$

and consequently we have:

$$\zeta_{eff} = \varphi_o + \alpha \sinh^2\left(\frac{Fz\varphi_o}{2RT}\right) \quad (2.22)$$

where:

$$\alpha = 4 \frac{C_b RT}{FzC_m}$$

---

It is also noteworthy that in the Debye-Huckel regime the last equation can be approximated by:

$$\zeta_{eff} \simeq \varphi_o + \beta \varphi_o^2$$

in which  $\beta = \frac{C_b F Z}{C_m R T}$  and thus clearly a nonlinear quadratic relation between  $\zeta_{eff}$  and the interfacial potential,  $\varphi_o$ , is predicted by "Bazant's jamming effect hypothesis".

2.2.3 *A reformulation of electrokinetic flow by Bingham-type fluid  
mechanics analysis*

Engineers and scientists are quite familiar with the concept of frictional force in simple physics problems. This principle simply indicates that if there is any relative motion of an object with respect to the surface on which it rests, then there is a corresponding friction force which is proportional to the normal force " $N$ " exerted by the surface on the object. However we usually do not think of frictional shear components in Solid Mechanics. This becomes clear when we note that in the constitutive laws of elasticity, the shear stress are independent of the normal stress components.

Classical Fluid Mechanics constitutive laws have probably been motivated by their predecessors in solid mechanics. Basically, the only difference between Fluid and Solid Mechanics is that in Fluid Mechanics "*strain rate*" has replaced "*strain*" in stress-strain relationships in elasticity.

Interestingly, a special type of non-Newtonian fluid called "Bingham plastic", [22–26], shows a typical behavior that is reminiscent of a high school Dynamics problem with non negligible friction force terms, namely that a block under an external force, does not move unless the force exceeds a threshold which is given as  $F_{th} = \mu_s N$ . Likewise the Bingham plastic does not experience any shear strain rate unless the shear stress exceeds a yield value.

Motivated by the above analogy, if we assume that in a continuum body the shear stress is also proportional to the normal stress components, e.g pressure in fluids, we can see that if there is a considerable gradient in the pressure distribution profile, then on any infinitesimal block of fluid there is a net friction type force which opposes fluid flow.[Fig.2.1]

As shown in Figure(2.1), one special case where large gradients in the pressure profile are present, occurs inside the double layer where the pressure field exponentially decreases as one goes from the wall surface through the bulk of fluid. The presence of these friction-type shear forces may explain the over prediction of zeta potential in ICEO experiments as pointed out in [21].

In what follows, I propose a general constitutive law for a Newtonian fluid with frictional stress components and then continue with application of the idea to the simple planar electroosmotic flow.

The classical constitutive law for finding stresses in terms of strain rates is:

$$\sigma_{ij} = -P\delta_{ij} + \eta\gamma_{ij}$$

where  $\gamma_{ij}$  is given as:

$$\gamma_{ij} = \frac{1}{2}(u_{i,j} + u_{j,i})$$

Motivated by the aforementioned observation, I propose a more general constitutive law which only adds an extra term to the above equation:

$$\boldsymbol{\sigma} = -P\mathbf{I} + \eta\gamma_{ij} \mathbf{e}_i \otimes \mathbf{e}_j + b_{ij} \mathbf{b}_i \otimes \mathbf{b}_j \quad (2.23)$$

In this formulation  $\mathbf{b}_i$  refers to a vector basis in which  $\mathbf{b}_1$  is the unit vector in the direction of net body force at a particular point and  $\mathbf{b}_2$  &  $\mathbf{b}_3$  are constructed as such to form a right handed set of orthogonal basis with  $\mathbf{b}_1$ . Moreover  $b_{12} = b_{21} = b_{13} = b_{31} = P\mu$  where  $\mu$  is the friction coefficient and other components are zeros.

Now if we plot shear stress as a function of strain rates, using the newly proposed constitutive law, we get a straight line with a finite intercept which is exactly what the Bingham formulation predicts. This indeed reminds us again of the analogy of the transition from sliding to kinetic friction in basic Dynamics problems.

With the above insight, we continue to see the mathematical implications of this hypothesis in simple planar electrokinetic flows. In accordance with figure(2.1), we introduce the following parameters:

Parameter	Description
$P$	Pressure
$\varphi$	Electric potential field
$E_n$	Normal component of electric field: $\frac{\partial \phi}{\partial n}$
$\rho_e$	Electric charge density
$\mu_k$ & $\mu_s$	kinetic and static friction coefficients respectively
$\delta A$	area of the element under study
$\delta y$	a length increment in the normal direction

Momentum equation in  $y$  direction gives:

$$\begin{aligned} \delta A (P - (P + \delta P)) + \rho_e E_n \delta A \delta y - \rho g \delta A \delta y &= 0 \Rightarrow \\ \delta P &= \rho_e E_n \delta y - \rho g \delta y \end{aligned} \quad (2.24)$$

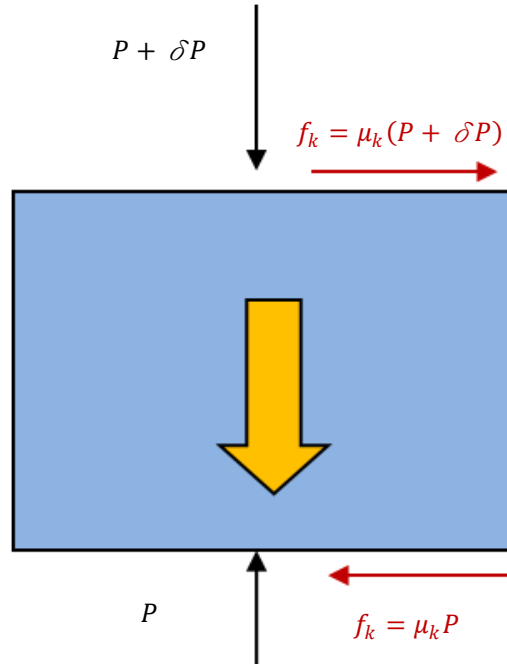


Fig. 2.1: friction forces on an infinitesimal fluid element in double layer

The net friction-type force acting on the body (see [Fig.2.1]) is now equal to  $\mu_k \delta P$ , we can safely neglect the variations in  $\delta P$  due to gravity because it is orders of magnitude less than that of normal electric field gradient, so that finally we have  $f_k$  equal to :

$$f_k = \mu_k \rho_e E_n \delta A \delta y = \mu_k \rho_e E_n \delta V \quad (2.25)$$

where  $\delta V$  refers to the volume of the element under consideration, this shows that the effect of frictional shear forces can be represented by a new body force term exerted into the classical Navier-Stokes equations:

$$\rho \left( \frac{\partial \mathbf{v}}{\partial t} + \mathbf{v} \cdot \nabla \mathbf{v} \right) = -\nabla P + \eta \nabla^2 \mathbf{v} + \mathbf{B} \quad (2.26)$$

Which in turn in the low Reynolds number regime simplifies to :

$$-\nabla P + \eta \nabla^2 \mathbf{v} + \mathbf{B} = 0 \quad (2.27)$$

Now assuming that there is no pressure gradient along the channel and using Poisson law for writing  $\rho_e$  in terms of gradients of electric potential field, we have:

$$\eta \nabla^2 \mathbf{v} + \mu_k \epsilon \nabla^2 \varphi \cdot \nabla \varphi - \epsilon E_{ext} \nabla^2 \varphi = 0$$

If we assume that the radius of curvature of the surface is much larger than the Debye length, then we can treat this problem as a planner one and get:

$$\eta \frac{\partial^2 v}{\partial y^2} + \mu_k \epsilon \frac{\partial^2 \varphi}{\partial y^2} \frac{\partial \varphi}{\partial y} - \epsilon E_{ext} \frac{\partial^2 \varphi}{\partial y^2} = 0 \quad (2.28)$$

Integration of this equation twice, and applying the no-slip boundary condition at  $y = 0$  gives:

$$v = -\frac{\mu_k \epsilon}{2\eta} \int_0^y \varphi(\tau)'^2 d\tau + \frac{\epsilon E_{ext}}{\eta} \varphi(y) - \frac{\epsilon E_{ext} \varphi_o}{\eta}$$

Consequently the bulk fluid velocity is found to be:

$$v_B = -\frac{\mu_k \epsilon}{2\eta} \int_0^\infty \varphi(\tau)'^2 d\tau - \frac{\epsilon E_{ext} \varphi_o}{\eta}$$

The Integral term in the above equation has been previously calculated in this work in the section on streaming potential measurements of  $\zeta$ , using the result of that calculation we get:

$$v_B = -\frac{\epsilon E_{ext}}{\eta} \varphi_o - \frac{4\mu_k \epsilon R^2 T^2}{F^2 \eta \lambda_D} \sinh^2 \left( \frac{F \varphi_o}{4RT} \right)$$

Now as usual by defining "effective zeta potential" ,  $\zeta_{eff}$  to be:

$$\zeta_{eff} = -\frac{\eta V_b}{\epsilon E_{ext}} \quad (2.29)$$

we get:

$$\zeta_{eff} = \varphi_o + \frac{4\mu_k R^2 T^2}{F^2 E_{ext} \lambda_D} \sinh^2 \left( \frac{F \varphi_o}{4RT} \right)$$

which in the Debye-Huckel regime can be further simplified to:



$$\zeta_{eff} \simeq \varphi_o + \frac{\mu_k \varphi_o^2}{4\lambda_D E_{ext}}$$

It is very interesting to note that in both the exact and Debye-Huckel approximations, the equations relating  $\zeta_{eff}$  to  $\varphi_o$  here, have the exact same functional form as the ones derived in an earlier section by using M.Bazant's proposed dependence of viscosity to charge density in the double layer [21]. Another interesting point is that the model presented here, in its current formulation, also predicts the possibility of flow reversal at extremely large voltages which has been experimentally observed in ICEO experiments [21], [11].

### 3. EXPERIMENTAL INVESTIGATION OF ELECTROOSMOSIS

#### *3.1 Streaming potential, a more accurate formulation*

Streaming potential is a well documented way of measuring zeta potential in micro-capillaries and along with current monitoring, has been extensively used as standard technique in electroosmotic experiments by different researchers over the decades.

The classical equation that has been used for inferring zeta potential from the observable parameter in the experiment (i.e voltage drop along the channel) is the solution of a much simplified model of the phenomenon. This simplified formulation may lead to inconsistencies between streaming potential and current monitoring measurements of zeta potential if used in the regimes where the simplifying assumptions break down.

In this section it is shown that in fact a more rigorous study of this phenomenon reveals a more complicated relationship between the observable voltage difference along the channel and zeta potential and that the first order approximation may in fact lead to significant error in estimating zeta potential.

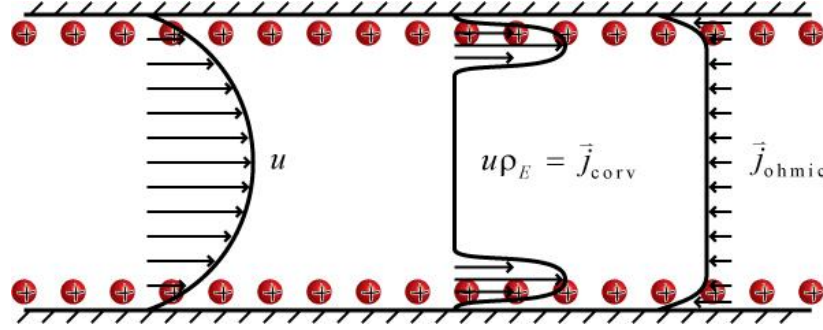
Since the technique has been extensively reviewed elsewhere [27–29], a very brief discussion of the phenomenon is first presented and is then immediately followed by the rigorous mathematical treatment of the problem.

As shown in figure(3.1), when a pressure gradient is applied along the channel, there would be a net migration of charged ions at the surface by fluid flow which then induces an electrical current in the channel. However if the channel is in an open circuit, there should be no net current flowing throughout the channel at the steady state.

Thus the steady state occurs when a voltage difference develops along the channel that produces an equal (Ohmic) current in the opposite direction. It has been shown [27] that this voltage difference should be equal to:

$$V = -\frac{\varphi_o \epsilon \nabla P}{\sigma \eta}$$

where  $\sigma$  is the bulk conductivity of the solution,  $V$  is the potential difference per unit length, and the other terms have their usual meanings, replacing  $\varphi_o$  by  $\zeta$  results in:



Courtesy of Brian Kirby

Fig. 3.1: Streaming potential phenomenon

$$\zeta = -\frac{\sigma\eta}{\epsilon\nabla P}V \quad (3.1)$$

which is the classical equation for relating streaming potential measurements to zeta potential of the substrate. There are two important simplifications made in deriving this equation:

1. *When a voltage difference is developed along the channel there will be an electroosmotic contribution to the fluid velocity which has been neglected in calculating the streaming current in above derivation*
2. *Since the concentration of ions varies greatly from their bulk values near the surface, there is an error associated with using bulk conductivity in calculation of Ohmic current*

In what follows we will consider both these facts and we will come up with a nonlinear relationship between the streaming potential and  $\zeta$ .

For a rectangular capillary of unit width and height of  $2h \gg 2\lambda_D$  the velocity field in bottom half of the channel is given as:

$$U_w = \frac{\epsilon E(\varphi - \varphi_0)}{\eta} + \frac{\nabla P}{2\eta} (y^2 - 2hy) \quad (3.2)$$

where  $E$  is the tangential electric field,  $y$  shows distance from the wall,  $\varphi$  is the potential at any particular point.

Furthermore the total net streaming current  $I_{str}$  is given as:

$$I_{str} = \int_0^h \rho_e U_w dA = -\epsilon \int_0^h \nabla^2 \varphi U_w dy \quad (3.3)$$

combining equations(3.2) and (3.3) we get:

$$I_{str} = I_1 + I_2$$

where

$$I_1 = -\frac{\epsilon^2 E}{\eta} \int_0^h \varphi'' (\varphi - \varphi_o) dy$$

$$I_2 = -\frac{\epsilon \nabla P}{2\eta} \int_0^h \varphi'' (y^2 - 2hy) dy$$

Using integration by parts yields:

$$\int_0^h (\varphi - \varphi_o) \varphi'' dy = \underbrace{\varphi' (\varphi - \varphi_o) \Big|_0^h}_0 - \int_0^h \varphi'^2 dy$$

The integral on the right side of the above equation can be calculated by using the general solution for P.B [27] equation which is known to be [12]:

$$\varphi = 2b \ln \left( \frac{1 + a \exp(\frac{-y}{\lambda_D})}{1 - a \exp(\frac{-y}{\lambda_D})} \right) \quad (3.4)$$

In which  $b = \frac{RT}{F}$  and  $a = \tanh(\frac{F\varphi_o}{4RT})$ . Differentiating with respect to  $y$  gives:

$$\varphi' = \frac{-4ab}{\lambda_D} \frac{\exp(\frac{-y}{\lambda_D})}{1 - a^2 \exp(\frac{-2y}{\lambda_D})}$$

so that we have:

$$\int_0^h (\varphi')^2 dy = \frac{16a^2b^2}{\lambda_D^2} \int_0^h \frac{\exp(\frac{-2y}{\lambda_D})}{(1 - a^2 \exp(\frac{-2y}{\lambda_D}))^2} dy = \frac{8b^2}{\lambda_D} \int_0^h \frac{\frac{2a^2}{\lambda_D} \exp(\frac{-2y}{\lambda_D})}{(1 - a^2 \exp(\frac{-2y}{\lambda_D}))^2} dy$$

By introducing a new variable  $u = 1 - a^2 \exp(\frac{-2y}{\lambda_D})$  the above integration simplifies to:

$$\int_0^h (\varphi')^2 dy = \frac{8b^2}{\lambda_D} \int_{1-a^2}^1 \frac{1}{u^2} du = \frac{8b^2a^2}{\lambda_D(1-a^2)}$$

Thus finally  $I_1$  is equal to:

$$I_1 = \frac{8\epsilon^2b^2a^2E}{\lambda_D\eta(1-a^2)} \quad (3.5)$$

$I_2$  can be approximated by using integration by parts and employing Debye-Huckel limit for the very last integrand,

$$\int_0^h \varphi'' (y^2 - 2hy) dy = \underbrace{\varphi' (y^2 - 2hy) \big|_0^h}_0 - 2 \int_0^h \varphi' (y - h) dy$$

$$\int_0^h \varphi' (y - h) dy = \varphi (y - h) \big|_0^h - \int_0^h \varphi dy \Rightarrow$$

$$\int_0^h \varphi'' (y^2 - 2hy) dy = -2\varphi_0 (-h + \lambda_D) \simeq 2\varphi_0 h$$

so that finally

$$I_2 = -\frac{\epsilon \nabla P h}{\eta} \varphi_o \quad (3.6)$$

Combining equations 3.3 to 3.6 yields:

$$I_{str} = -\frac{\epsilon \nabla P h}{\eta} \varphi_o + \frac{8\epsilon^2 b^2 a^2 E}{\lambda_D \eta (1 - a^2)} \quad (3.7)$$

Ohmic current basically occurs as a result of electrophoretic migration of ions in the solution, if we show mobility and concentration of cations by  $\mu_+$  and  $C_+$  respectively and those of anions by  $\mu_-$  and  $C_-$  then:

$$I_{ohm} = EF \left( \int_0^h \mu_+ C_+ dy + \int_0^h \mu_- C_- dy \right) = EFC_o \mu \int_0^h \left( \exp\left(\frac{-F\varphi}{RT}\right) + \exp\left(\frac{F\varphi}{RT}\right) \right) dy$$

furthermore if we assume that cation and anions have similar mobilities, the above equation yields:

$$I_{ohm} = 2EFC_o \mu \int_0^h \left( \cosh\left(\frac{F\varphi}{RT}\right) \right) dy \quad (3.8)$$

But if we multiply both sides of P.B equation [12], by  $\varphi'$  and then integrate, we get:

$$\int_0^h \varphi' \varphi'' dy = \int_0^h \frac{2C_b F}{\epsilon} \sinh\left(\frac{F\varphi}{RT}\right) \varphi' dy \Rightarrow$$

$$\varphi'^2 = \frac{4C_b RT}{\epsilon} \left( \cosh\left(\frac{F\varphi}{RT}\right) - 1 \right) \Rightarrow$$

$$\int_0^h \cosh\left(\frac{F\varphi}{RT}\right) dy = \frac{\epsilon}{4C_b RT} \int_0^h \varphi'^2 dy + h = \frac{2\epsilon b^2 a^2}{C_b RT \lambda_D (1 - a^2)} + h$$

So that finally by realizing  $\sigma = 2\mu C_b F$

$$I_{ohm} = \sigma E h \left( 1 + \frac{2\epsilon b^2 a^2}{C_b RT \lambda_D h (1 - a^2)} \right) \quad (3.9)$$

Also it is useful to note that:

$$\frac{a^2}{1 - a^2} = \frac{1}{\frac{1}{a^2} - 1} = \frac{1}{\coth\left(\frac{F\varphi_o}{4RT}\right)^2 - 1} = \sinh^2\left(\frac{F\varphi_o}{4RT}\right)$$

As previously mentioned, at steady state the net current should be zero which means:

$$I_{total} = I_{str} + I_{ohm} = 0$$

$$-\sigma V h - \frac{\epsilon \nabla P h}{\eta} \varphi_o - \sigma V h \left( \frac{2\epsilon b^2}{C_b RT \lambda_D h} + \frac{8\epsilon^2 b^2}{\lambda_D \eta \sigma h} \right) \sinh^2\left(\frac{F\varphi}{4RT}\right) = 0$$

$$\zeta = \frac{\varphi_o}{1 + \left( \frac{2\epsilon b^2}{C_b RT \lambda_D h} + \frac{8\epsilon^2 b^2}{\lambda_D \eta \sigma h} \right) \sinh^2\left(\frac{F\varphi}{4RT}\right)}$$



3.2 *Current monitoring measurement of zeta in Silica  
micro-capillaries*

3.2.1 *A new data set for Silica micro-capillary for alkaline buffers*

During the course of working on this project, I found few experimental data available for  $\zeta$  potential measurements of different buffers with high salt concentration for silica microchannels. Furthermore, I believe that it is in these extreme regimes (low or high salt concentration, pH, etc) where we can get valuable insight as to whether or not the current models can explain different aspects of the phenomenon suitably. I then decided to conduct a number of careful experiments at high salt concentrations myself to investigate the robustness of proposed models in this work and to provide reliable data for future academic investigations.

I decided to conduct a series of "current monitoring" experiments in which our group has a good experience and expertise. The current monitoring technique has been well discussed elsewhere and the interested reader is encouraged to look in the literature for more details [27, 30, 31].

In our experimental setup we have been careful to avoid error sources associated with current monitoring technique as discussed in [32, 33]. Specially we took care of Joule heating effects in the sense that whenever we observed continuous growth in zeta potential during the course of experiment, we attributed that to the decrease in the viscosity of the fluid due to Joule heating effects and hence disregarded the data set as unreliable. We were also careful to avoid more than 5-7.5 % difference in the two electrolyte buffer conductivities to avoid axially non-uniform interfacial potential and voltage drop inside the capillary, both of which result in pressure driven flow being developed.

In this section, I have included both the raw and processed experimental data. I will use the data in the next section along with other data sets available in the literature to investigate different aspects of the Electrochemical and the various Fluid Mechanics models presented in previous sections. The raw graphs are also presented because they show the extent to which our data set is reliable.

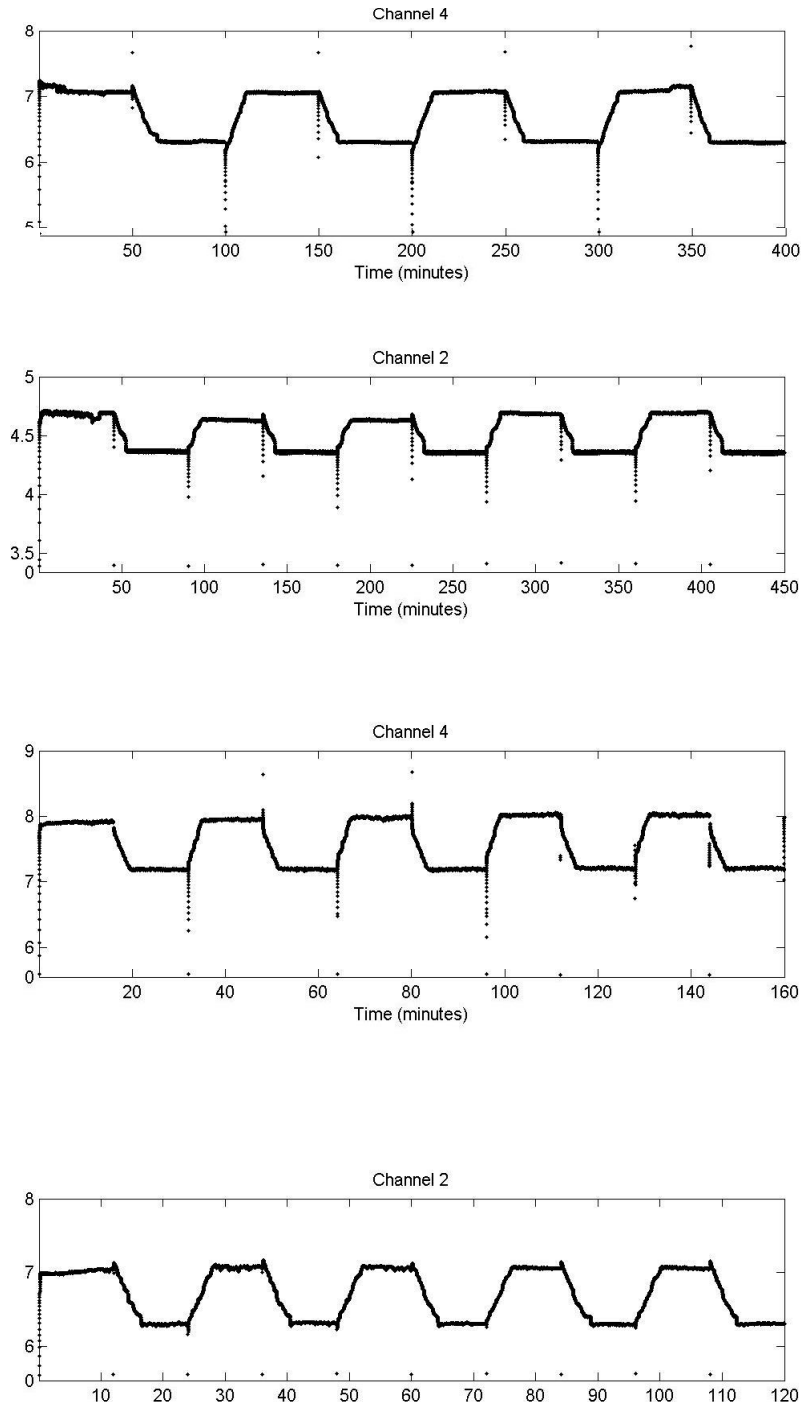


Fig. 3.2: Current monitoring raw data for 1M solution, pH=4.1 , 5 , 6 , 7

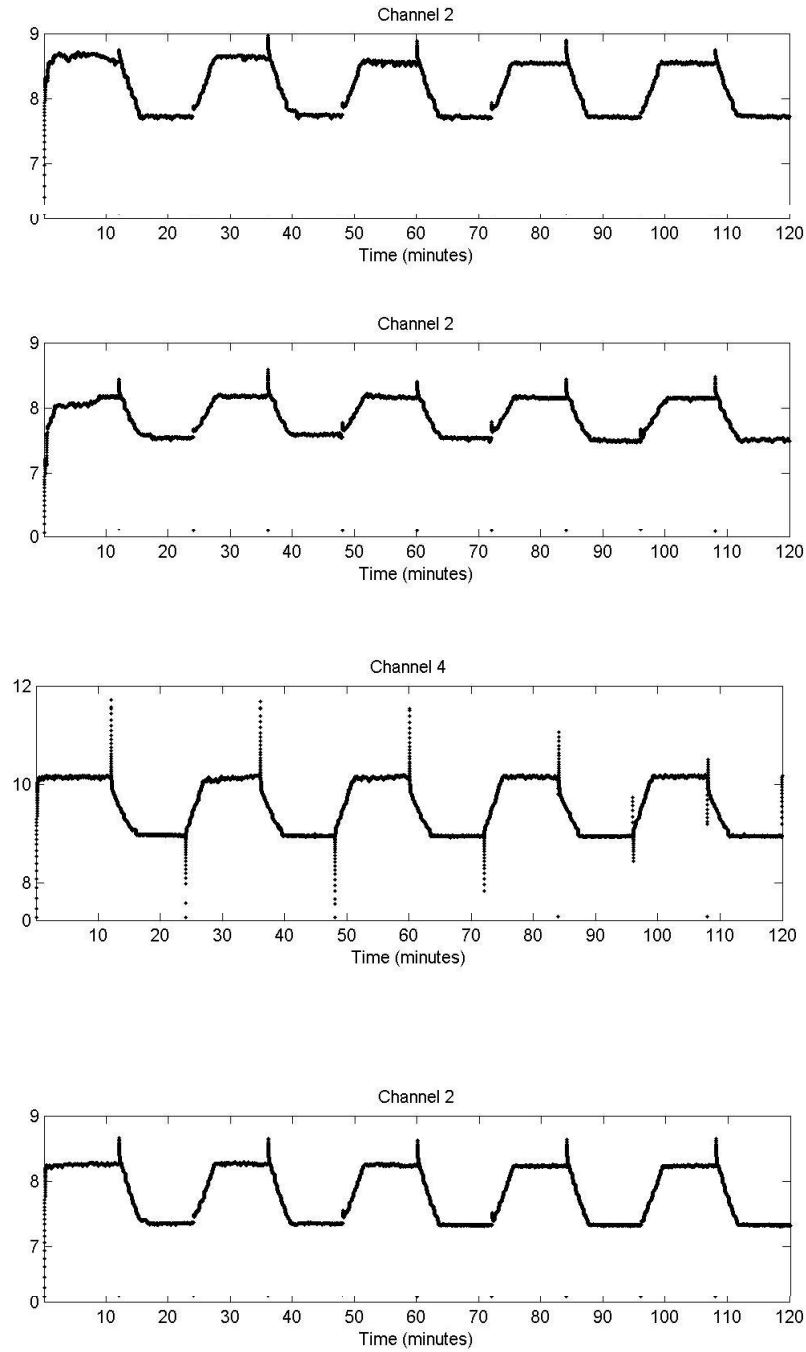


Fig. 3.3: Current monitoring raw data for 1M solution, pH=8 , 9 , 10 , 11

Zeta potential measurements 1M phosphate buffer Silica capillary		
pH	Zeta potential (mV)	Standard deviation (mV)
4.1	-4.67	0.26
5	-9.47	1.62
6	-17.6	1.65
7.1	-17.92	0.67
8	-19.4	2.3
9	-21.7	2.41
10	-24	1.68
11	-23.9	2.25

*Fig. 3.4:* Processed data for 1M phosphate buffer

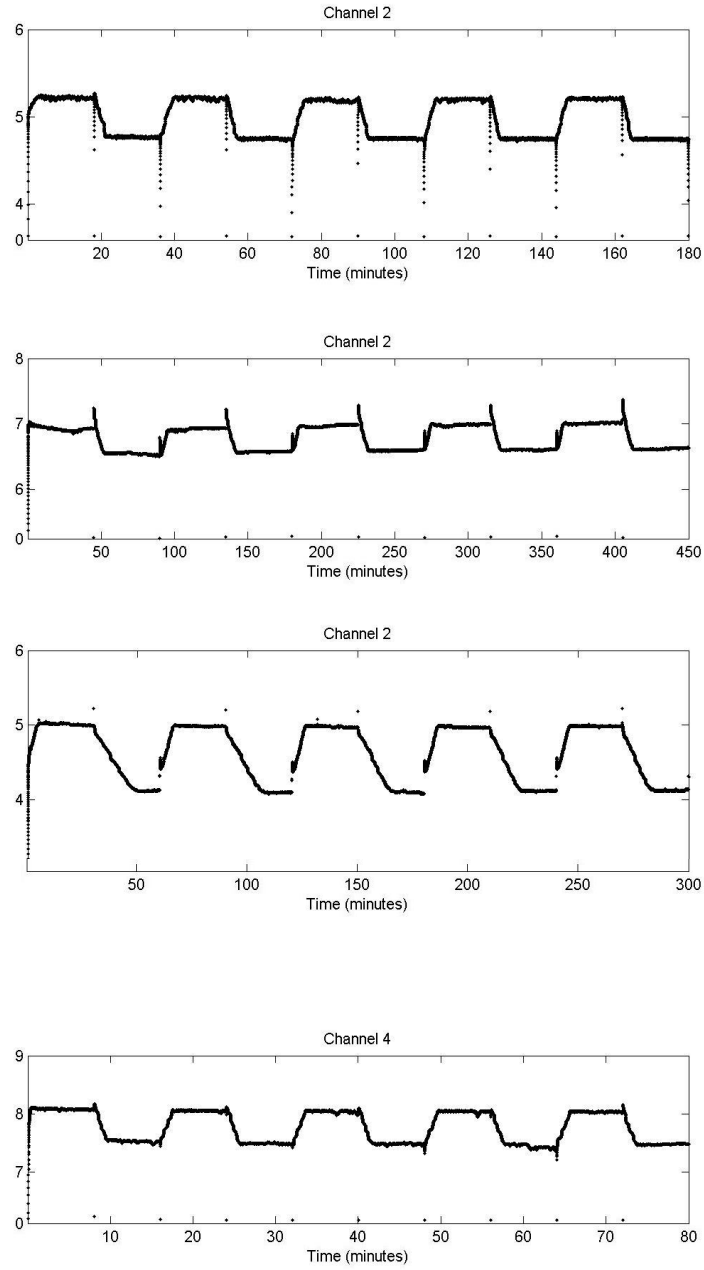


Fig. 3.5: Current monitoring raw data for 100mM solution, pH=4.3, 5.6, 6.6, 8

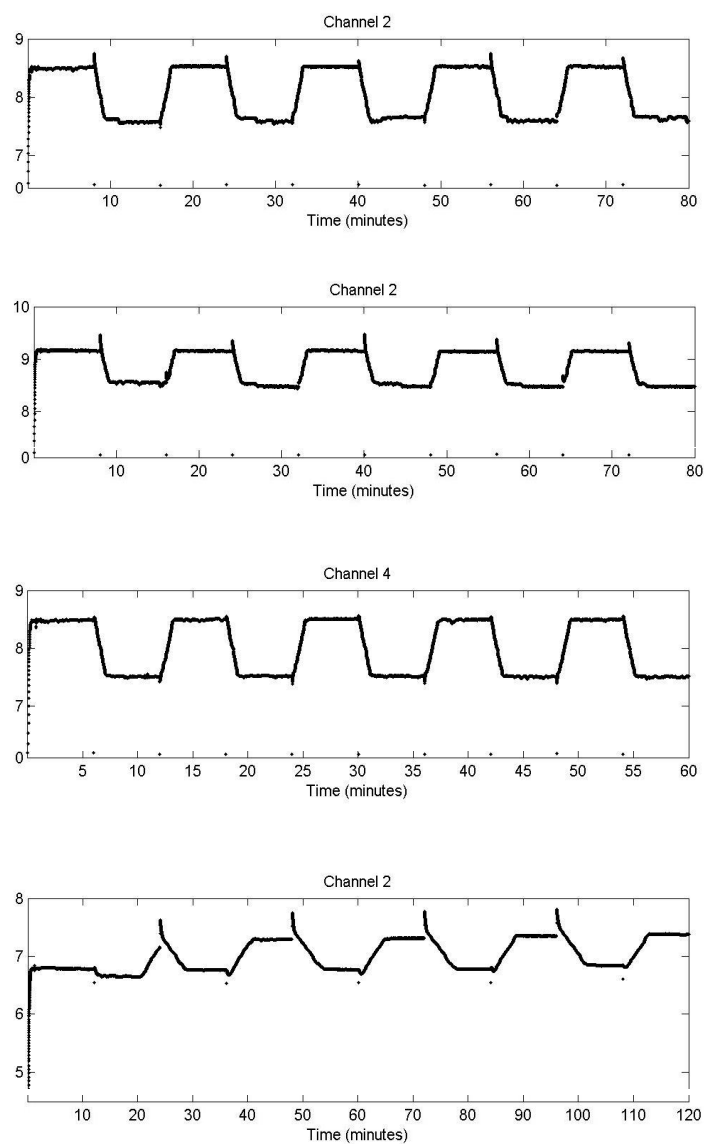


Fig. 3.6: Current monitoring raw data for 100mM solution, pH=9, 10, 11.3, 12.4

Zeta potential measurements 100mM phosphate buffer Silica capillary		
pH	Zeta potential (mV)	Standard deviation (mV)
4.3	-15.64	2.7
5.5	-23.11	2
6.6	-33.65	2.31
8	-43.57	2.52
9	-52.1	2.60
10	-55.52	3.4
11.3	-61.2	1.52
12.4	-55.9	0.28

*Fig. 3.7:* Processed data for 100mM phosphate buffer



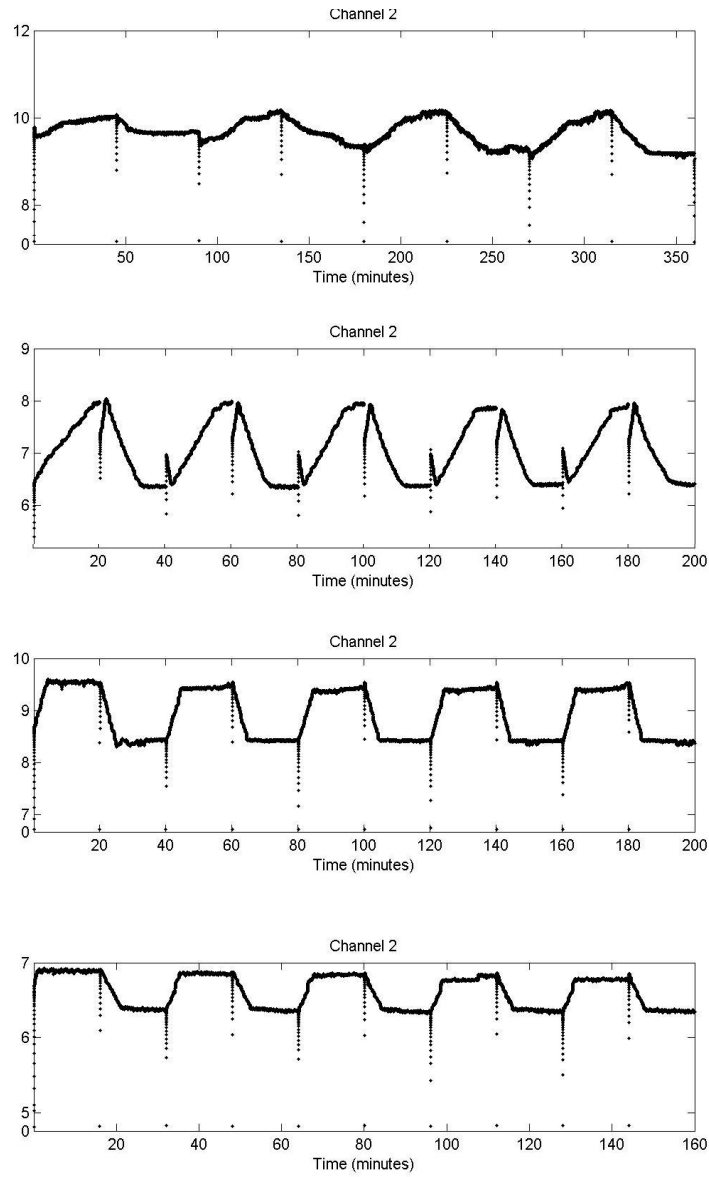


Fig. 3.8: Current monitoring raw data for 10mM solution, pH=3.3, 4.6, 5.6, 6.6

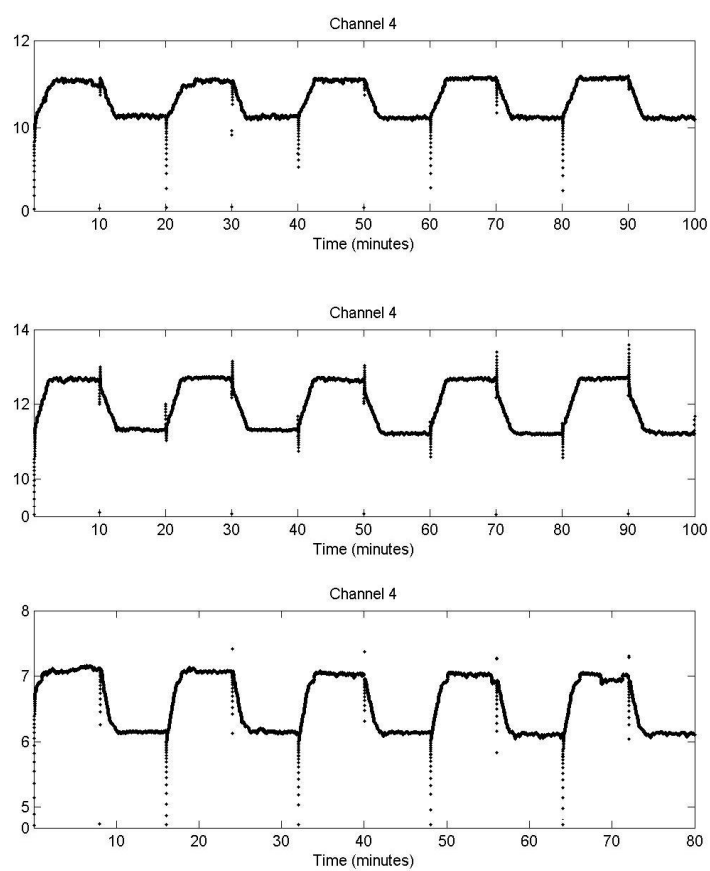


Fig. 3.9: Current monitoring raw data for 10mM solution, pH=7, 8.5, 11.4

Zeta potential measurements 10mM phosphate buffer Silica capillary		
pH	Zeta potential (mV)	Standard deviation (mV)
3.3	-5.08	0.76
4.6	-15.53	1.88
5.6	-31.26	5.22
6.6	-52.35	7.78
7	-57.18	5.82
8.6	-65.63	4.17
11.6	-83.27	6.30

Fig. 3.10: Processed data for 10mM phosphate buffer

Finally before concluding this section, I would like to point out an interesting result about the increase in the pressure field inside the solution due to presence of electrostatic forces in the double layer. This new insight can potentially lead to new experimental techniques for zeta (more accurately interfacial) potential measurements.

In the low Reynolds regime the classical Navier-Stokes equation gives:

$$-\nabla P + \eta \nabla^2 \mathbf{v} + \mathbf{B} = 0 \quad (3.10)$$

Now in a planar geometry, If we assume that the fluid velocity components in the "y" direction, i.e normal to capillary surface, is zero or at most linear in  $y$ , and we insert the existing body force terms in the above equation we have:

$$\frac{\partial P}{\partial y} = \epsilon \frac{\partial^2 \varphi}{\partial y^2} \frac{\partial \varphi}{\partial y} - \rho g$$

If we integrate the above equation from the channel surface to the bulk of fluid, say " $h$ " meters above the surface, pressure difference is:

$$P_s - P_b = \frac{\epsilon}{2} E_n^2 + \rho g h \quad (3.11)$$

Where  $P_s$  and  $P_b$  show pressures at the surface and the bulk of fluid respectively,  $E_n$  is the normal component of electric field at the surface and the  $\rho g h$  is the familiar gravitational contribution to the pressure field. The first term on the right hand side of the above equation is due to electrostatic forces present in the double layer. We can get an estimate of the order of this number in by using Debye-Huckel approximation:

$$\varphi \simeq \varphi_o \exp\left(-\frac{y}{\lambda_D}\right) \Rightarrow \quad (3.12)$$

$$E = -\frac{\partial \varphi}{\partial y} \simeq \frac{\varphi_o}{\lambda_D} \exp\left(-\frac{y}{\lambda_D}\right) \Rightarrow \quad (3.13)$$

$$\frac{\epsilon}{2} E_n^2 \simeq \frac{\epsilon \varphi_o^2}{2 \lambda_D^2} \quad (3.14)$$

If we use typical values of  $\varphi = 25mV$  and  $\lambda_D = 3nm$  we get that excess pressure to be around:

$$\frac{\epsilon \varphi_o^2}{2 \lambda_D^2} \simeq 25 KPa$$

The excess pressure is thus a relatively large number. Unfortunately measuring this excess pressure is not straightforward. For example if we try to calculate the pressure by measuring the force exerted on the channel surface we get a null result. The reason is that the surface itself is charged and an exact and opposite electrostatic force balances out the force exerted by the fluid pressure field on the surface. Another issue is that this phenomenon is observable near the double layer region which is only few nanometers away from the surface, thus a typical pressure transducer can not be used to measure this excess potential accurately. There may be other ways to take advantage of this excess pressure to measure zeta potential. Exploring ways to implement the idea presented here for  $\zeta$  potential measurements can be a candidate for future research endeavors in the field.

3.2.2 *A proposed  $\zeta$  potential measurement method based on excess electrostatic pressure in the double layer*

Before concluding this section, I would like to point out an interesting result about the increase in the pressure field inside the solution due to presence of electrostatic forces in the double layer. This new insight can potentially lead to new experimental techniques for zeta (more accurately interfacial) potential measurements.

In the low Reynolds regime the classical Navier-Stokes equation gives:

$$-\nabla P + \eta \nabla^2 \mathbf{v} + \mathbf{B} = 0 \quad (3.15)$$

Now in a planar geometry, If we assume that the fluid velocity components in the "y" direction, i.e normal to capillary surface, is zero or at most linear in  $y$ , and we insert the existing body force terms in the above equation we have:

$$\frac{\partial P}{\partial y} = \epsilon \frac{\partial^2 \varphi}{\partial y^2} \frac{\partial \varphi}{\partial y} - \rho g$$

If we integrate the above equation from the channel surface to the bulk of fluid, say " $h$ " meters above the surface, pressure difference is:

$$P_s - P_b = \frac{\epsilon}{2} E_n^2 + \rho g h \quad (3.16)$$

Where  $P_s$  and  $P_b$  show pressures at the surface and the bulk of fluid respectively,  $E_n$  is the normal component of electric field at the surface and the  $\rho g h$  is the familiar gravitational contribution to the pressure field. The first term on the right hand side of the above equation is due to electrostatic forces present in the double layer. We can get an estimate of the order of this number in by using Debye-Huckel approximation:

$$\varphi \simeq \varphi_o \exp\left(-\frac{y}{\lambda_D}\right) \Rightarrow \quad (3.17)$$

$$E = -\frac{\partial \varphi}{\partial y} \simeq \frac{\varphi_o}{\lambda_D} \exp\left(-\frac{y}{\lambda_D}\right) \Rightarrow \quad (3.18)$$

$$\frac{\epsilon}{2} E_n^2 \simeq \frac{\epsilon \varphi_o^2}{2 \lambda_D^2} \quad (3.19)$$

If we use typical values of  $\varphi = 25mV$  and  $\lambda_D = 3nm$  we get that excess pressure to be around:

$$\frac{\epsilon \varphi_o^2}{2 \lambda_D^2} \simeq 25 KPa$$

The excess pressure is thus a relatively large number. Unfortunately measuring this excess pressure is not straightforward. For example if we try to calculate the pressure by measuring the force exerted on the channel surface we get a null result. The reason is that the surface itself is charged and an exact and opposite electrostatic force balances out the force exerted by the fluid pressure field on the surface. Another issue is that this phenomenon is observable near the double layer region which is only few nanometers away from the surface, thus a typical pressure transducer can not be used to measure this excess potential accurately. There may be other ways to take advantage of this excess pressure to measure zeta potential. Exploring ways to implement the idea presented here for  $\zeta$  potential measurements can be a candidate for future research endeavors in the field.



## 4. CONCLUSION

In this chapter, the model that was developed in the earlier sections, is used to study and explain various data sets, including our own experimental results, in the literature on zeta potential measurements for silica micro-capillaries. The important result is that **different data sets** are explained with a **single model** which consistently uses only **two**, perfectly meaningful parameters.

Previously, several researchers have addressed the problem of zeta potential determination with respect to electrolyte solution properties and found ways of explaining experimental data. [14, 34–37] However, there are important drawbacks with those efforts:

1. Ad-hoc fitting parameters are often used to explain the data.
2. The fitting parameters are used inconsistently to explain the available data, and change from one situation to another without any physical reasoning that explains why this should be allowed.
3. Usually a single data set has been explained with other available data sets being ignored.

I developed a MATLAB code based on my model for prediction of zeta potential in silica micro-capillaries in terms of chemical properties of solution, i.e the model presented in chapter II of this work and also wrote a simple optimization module which finds the optimum set of parameters to fit my model to available experimental data in the literature.

There were originally four fitting parameters in my model, two reaction equilibrium constants,  $K_1$  &  $K_2$ , a parameter for the number of Silanol sites at the glass surface,  $N_s$ , and an  $\alpha$  parameter which can be considered as the coefficient of the second term in the Taylor expansion of the relation between  $\zeta$  and  $(\varphi_o)$ .

The relation between interfacial and zeta potentials has been studied to some extent in an earlier chapter from a mere fluid mechanical point of view. There, it has been shown that at least three different physical models, proposed by different researchers, lead to non linear relations between bulk fluid velocity and interfacial potential. I thus introduced a general  $\alpha$  parameter in my optimization module to account for possible nonlinear relations

between  $\zeta$  and  $\varphi_o$ .

Since the proposed nonlinear relations appeared in Fluid Mechanics formulations of electroosmosis, the  $\alpha$  parameter was not used in explaining "streaming potential" data because the technique does not measure bulk electroosmotic fluid velocity and rather measures the interfacial potential. It should be noted that based on our studies of the streaming potential technique in an earlier chapter, we saw that in fact a nonlinear equation should be used for inferring zeta potential from measured voltage drop. However, the nonlinear correction terms turned out to be negligible for the data sets studied in this work.

My analysis of available data showed that only two of the original four fitting parameters ( $K_1$  &  $N_s$ ), are necessary to explain data and there is no strong evidence to motivate either cation binding hypothesis or nonlinear relationships between  $\zeta$  and  $\varphi_o$ , at least in the electric potential and flow regimes studied in this work.

Starting with metal cation binding, I observed that introducing a non-negligible equilibrium constant for this type of reaction,  $K_2$ , makes the model become inaccurate at high salt concentrations. There, the model predicts a constant, almost zero zeta potential regardless of pH and this is in complete disagreement with experimental observations[see figures below]. Moreover, at moderate salt concentrations, introducing  $K_2$  does not really improve accuracy of the model. As a result of these observations, I decided that  $K_2$  is a redundant parameter and hence equated it to zero in my code.

In other words I have concluded that metal cation reactive binding with Silica does not happen for alkaline(e.g  $K^+$ ,  $Na^+$ , ...) buffers. A possible intuitive explanation of this observation is that group **I** metals are not absorbed to silica strongly enough to penetrate the screening water layer on the silica surface. On the other hand, alkaline earth metals, i.e group **II** metals, are able to reach the Silica surface and react with or get absorbed to the surface. Not surprisingly, there is evidence supporting specific absorption and positive electrokinetic potential for divalent cation groups in the literature [38].

This conclusion is also consistent with a particularly illuminating data in the literature which compares different alkaline buffers zeta potential [39]. As shown in figure(4.3), we can see that there is no significant difference between measured zeta potential for  $Li^+$ ,  $Na^+$ ,  $K^+$  buffers. We can thus

---

conclude that either different alkaline buffer-Silica reactions all have roughly the same equilibrium constants, which is unlikely, or that simply those reactions do not occur because of the strong shielding of the Silica surface by water molecules as discussed above.

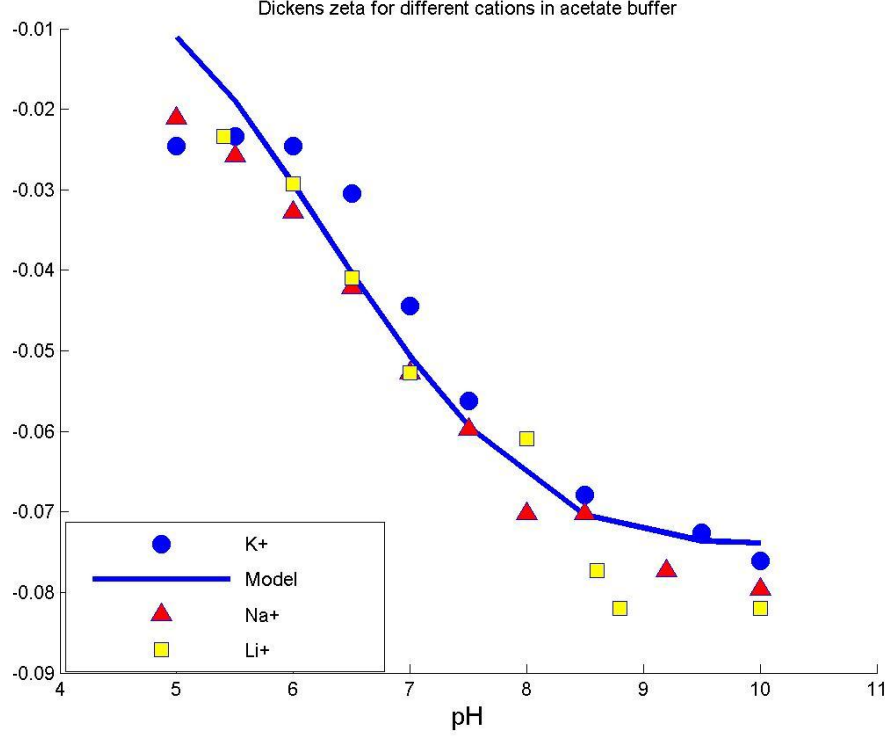


Fig. 4.1: Comparison between different group I metal cations

I also found that the classical Smoluchowski's formula can explain the majority of data sets studied here and that there is no evidence for a non-linear relation between electroosmotic velocity and  $\varphi_o$ . This translates to finding the  $\alpha$  parameter, as defined before, to be zero in the optimization process for data fitting.

My fitting analysis suggested that a good estimate for the average site density of Silanol groups,  $N_s$ , is  $0.3 \frac{\text{sites}}{\text{nm}^2}$ . I deliberately allowed  $N_s$  to vary slightly from one experiment to another because it is indeed possible to have different material properties as a result of different manufacturing processes in different experiments. Statistically speaking, I found that on average  $N_s \simeq 0.28 \frac{\text{sites}}{\text{nm}^2}$  with a standard deviation of  $\sigma_d = 0.13 \frac{\text{sites}}{\text{nm}^2}$ .

I also found that interestingly there are two different  $K_1$  values that

---

should be used to explain two distinct groups of available data. I attribute this to the possibility of having two main and different classes of silica capillaries with slightly different atomistic structures. This can account for having different equilibrium constant for deprotonation of silica substrate. The idea of having two or more different classes of Silicon is not unprecedented and there is evidence for having two main different classes of Silicon in the literature [12, 40]. Bousse and Mostarshed, observed shifts in the point of zero charge when Silicon with  $SiNH_4$  impurities was used instead of the usual  $SiH_2$  Silicon material.

Likewise, I found two equilibrium constant values to be  $K_1 \simeq 1.2 \cdot 10^{-3}$  and  $K_1 \simeq 4.7 \cdot 10^{-2}$  M and the numerical predictions of the presented model for the two different cases showed a shift in the iso-electric points from approximately 3 to 2 for 10mM  $KCl$  solution.

I have gathered the results of my investigations for different data sets in the below graphs and the the two tables that show the fitting parameters in the two distinct classes. It can be seen that the equilibrium constants in the tables are consistent with what presented above and acquires only two different values with the site density of Silanol groups varying (slightly) from experiment to experiment .

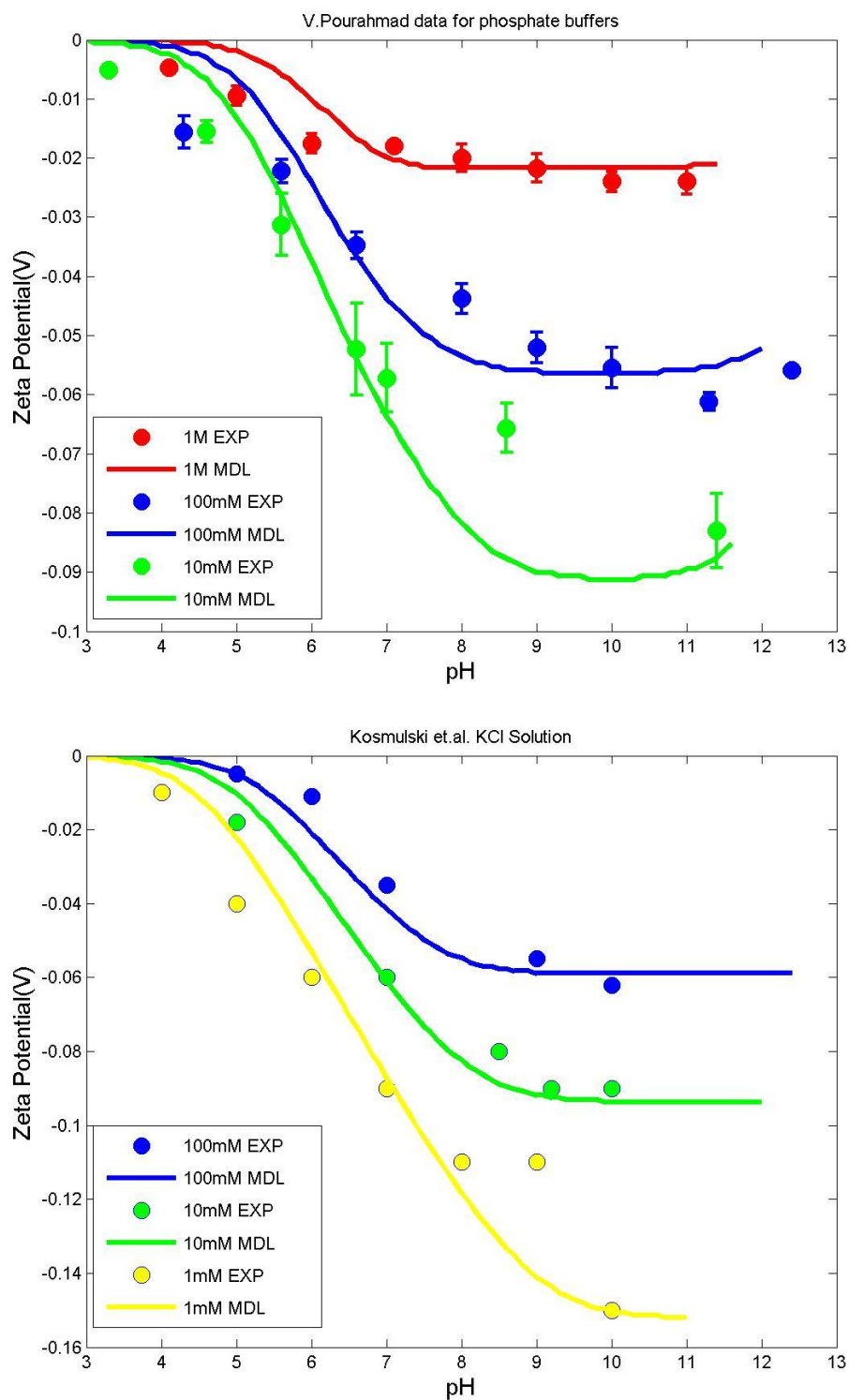


Fig. 4.2: Top: V.Pourahmad data Bottom:Kosmulski et al. [15]

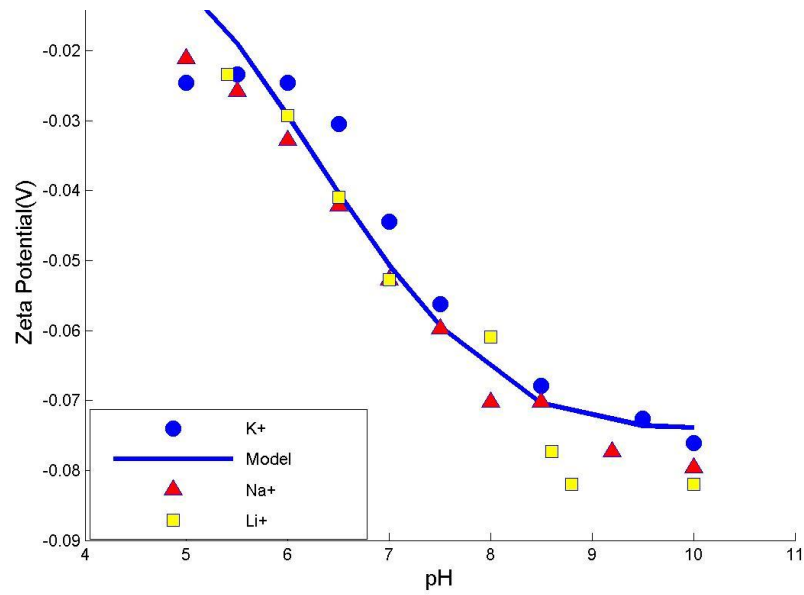


Fig. 4.3: Dickens et al. data [39]

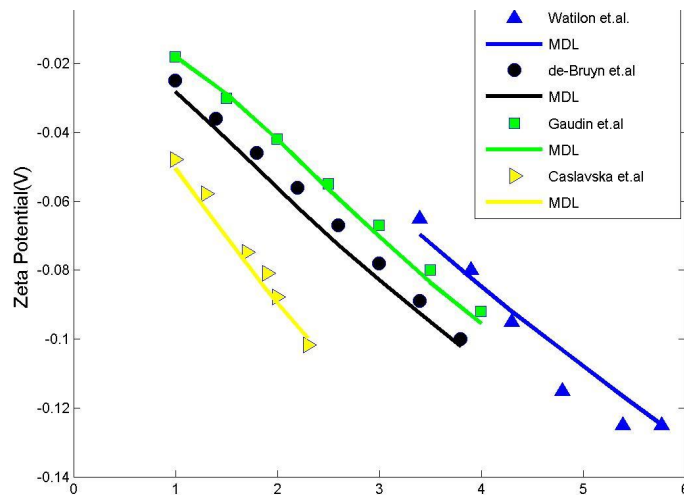


Fig. 4.4: Variation of zeta with salt concentration,[41–43]



Reference	$K_1$ ( $10^{-3}M$ )	$N_s$ (sites/nm <sup>2</sup> )
Kosmulski et.al. 100mM KCl solution	1.2	0.33
Kosmulski et.al. 10mM KCl solution	1.2	0.22
Kosmulski et.al. 1mM KCl solution	1.2	0.22
V.Pourahmad 1M phosphate buffer	1.2	0.5
V.Pourahmad 100mM phosphate buffer	1.2	0.45
V.Pourahmad 10mM phosphate buffer	1.2	0.3
Dickens et.al.	1.2	0.3
De-Bruyn et.al.	1.2	0.18
Watillon et.al.	1.2	0.06
Gaudin et.al.	1.2	0.1
Caslavska <sub>(b)</sub> et.al.	1.2	0.3

Fig. 4.5: Variation in site density of first Silica type groups

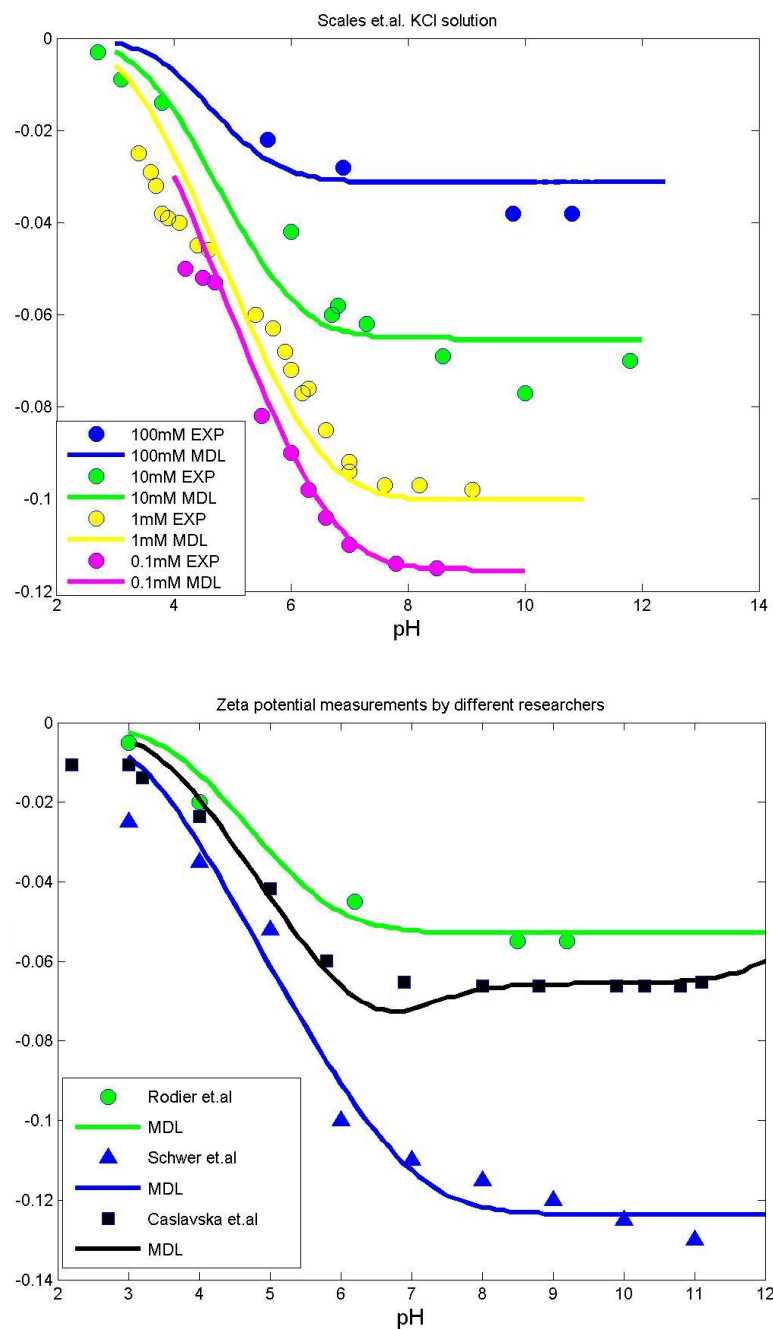


Fig. 4.6: Zeta potential measurements on silica by different researchers, [14, 43–45]

Reference	$K_1$ ( $10^{-2}M$ )	$N_s$ (sites/nm <sup>2</sup> )
Scales et.al. 100mM KCl solution	4.7	0.15
Scales et.al 10mM KCl solution	4.7	0.12
Scales et.al 1mM KCl solution	4.7	0.08
Scales et.al 0.1mM KCl solution	4.7	0.035
Caslavska et.al 40mM phosphate buffer	4.7	0.35
Schwer et.al 10mM KCl solution	4.7	0.4

Fig. 4.7: Variation in site density of type II silanol groups

## BIBLIOGRAPHY

- [1] A. K., S. K., and C. D., “Inkjet-printed microfluidic multianalyte chemical sensing paper,” *Anal.Chem.Analytical Chemistry*, vol. 80, no. 18, pp. 6928–6934, 2008. ID: 282997600.
- [2] S. G.J. and H. A.V., “Ief in microfluidic devices,” *Electrophoresis Electrophoresis*, vol. 30, no. 5, pp. 742–757, 2009. ID: 701172710.
- [3] L. IM, L. L, Y. Y, and K. BL, “Microfluidic device for capillary electrochromatography-mass spectrometry,” *Electrophoresis*, vol. 24, no. 21, pp. 3655–62, 2003. ID: 110394499.
- [4] S. A, E. D, R. L, and L. D, “Zeta-potential measurement using the smoluchowski equation and the slope of the current-time relationship in electroosmotic flow,” *Journal of colloid and interface science*, vol. 261, no. 2, pp. 402–10, 2003. ID: 111544339.
- [5] J. LYKLEMA and J. OVERBEEK, “On the interpretation of electrokinetic potentials,” *Journal of Colloid Science Journal of Colloid Science*, vol. 16, no. 5, pp. 501–512, 1961. ID: 4642535919.
- [6] E. N. da C. Andrade and C. Dodd, “The effect of an electric field on the viscosity of liquids,” *Proceedings of the Royal Society of London.Series A, Mathematical and Physical Sciences*, vol. 187, no. 1010, pp. 296–337, 1946. ID: 479044853.
- [7] E. N. da C. Andrade and C. Dodd, “The effect of an electric field on the viscosity of liquids. ii,” *Proceedings of the Royal Society of London.Series A, Mathematical and Physical Sciences*, vol. 204, no. 1079, pp. 449–464, 1951. ID: 479074084.
- [8] N. G. Green, A. Ramos, and H. Morgan, “Ac electrokinetics: a survey of sub-micrometre particle dynamics,” *Journal of physics.D: applied physics.*, vol. 33, pp. 632–641, 2000. ID: 104985244.

- 
- [9] V. Studer, A. Ppin, Y. Chen, and A. Ajdari, "An integrated ac electrokinetic pump in a microfluidic loop for fast and tunable flow control," *The Analyst*, vol. 129, no. 10, pp. 944–949, 2004. ID: 366616496.
- [10] T. M. SQUIRES and M. Z. BAZANT, "Induced-charge electroosmosis," *Journal of Fluid Mechanics*, vol. 509, no. 1, pp. 217–252, 2004. ID: 364097739.
- [11] M. Z. Bazant, M. S. Kilic, B. D. Storey, and A. Ajdari, "Towards an understanding of induced-charge electrokinetics at large applied voltages in concentrated solutions," *Advances in colloid and interface science.*, vol. 152, no. 1, p. 48, 2009. ID: 464553800.
- [12] K. BJ and H. E. Jr, "Zeta potential of microfluidic substrates: 1. theory, experimental techniques, and effects on separations.," *Electrophoresis*, vol. 25, no. 2, pp. 187–202, 2004. ID: 111777777.
- [13] T. V., B. S.K., N. W.C., and K. B.J., "Zeta potential and electroosmotic mobility in microfluidic devices fabricated from hydrophobic polymers: 1. the origins of charge," *Electrophoresis Electrophoresis*, vol. 29, no. 5, pp. 1092–1101, 2008. ID: 281899493.
- [14] P. J. Scales, F. Grieser, T. W. Healy, L. R. White, and D. Y. C. Chan, "Electrokinetics of the silica-solution interface: a flat plate streaming potential study," *Langmuir Langmuir*, vol. 8, no. 3, pp. 965–974, 1992. ID: 4664354842.
- [15] M. Kosmulski and E. Matijevic, "zeta-potentials of silica in water-alcohol mixtures," *Langmuir*, vol. 8, no. 4, pp. 1060–1064, 1992. ID: 4436271112.
- [16] W. M. Haynes and D. R. Lide, *CRC handbook of chemistry and physics : a ready-reference book of chemical and physical data*. Boca Raton, Fla.; London: CRC ; Taylor and Francis [distributor], 2010. ID: 540161491.
- [17] G. H. Bolt, "Analysis of the validity of the gouy-chapman theory of the electric double layer," *Journal of Colloid Science*, vol. 10, no. 2, pp. 206 – 218, 1955.
- [18] G. Barnes and I. Gentle, *Interfacial science : an introduction*. Oxford ; Toronto: Oxford University Press, 2005. ID: 300290059.
- [19] P. C. Hiemenz, *Principles of colloid and surface chemistry*. New York: M. Dekker, 1977. ID: 3186407.

- 
- [20] W. Schmickler, *Interfacial electrochemistry*. New York: Oxford University Press, 1996. ID: 32921712.
- [21]
- [22] H. Yamaguchi, “Engineering fluid mechanics,” 2008. ID: 233972603.
- [23] C. Tropea, A. L. Yarin, and J. F. Foss, “Springer handbook of experimental fluid mechanics,” 2007. ID: 213085432.
- [24] M. Chatzimina, G. C. Georgiou, I. Argyropaidas, E. Mitsoulis, and R. R. Huilgol, “Cessation of couette and poiseuille flows of a bingham plastic and finite stopping times,” *JOURNAL OF NONNEWTONIAN FLUID MECHANICS*, vol. 129, no. 3, pp. 117–127, 2005. ID: 210571426.
- [25] C. Y.-L. and Z. K.-Q., “Couette-poiseuille flow of bingham fluids between two porous parallel plates with slip conditions,” *J.Non-Newton.Fluid Mech.Journal of Non-Newtonian Fluid Mechanics*, vol. 153, no. 1, pp. 1–11, 2008. ID: 279575568.
- [26] Q. D. Nguyen and D. V. Boger, “Measuring the flow properties of yield stress fluids,” *Annual Review of Fluid Mechanics*, vol. 24, pp. 47–88, 1992. ID: 4761124313.
- [27] B. Kirby, *Micro- and nanoscale fluid mechanics : transport in microfluidic devices*. New York: Cambridge University Press, 2010. ID: 499130062.
- [28] D. Erickson and D. Li, “Streaming potential and streaming current methods for characterizing heterogeneous solid surfaces,” *Journal of colloid and interface science*, vol. 237, no. 2, pp. 283–289, 2001. ID: 359152835.
- [29] X. Xuan, “Streaming potential and electroviscous effect in heterogeneous microchannels,” *Microfluidics and Nanofluidics*, vol. 4, no. 5, pp. 457–462, 2008. ID: 437878049.
- [30] X. Huang, M. J. Gordon, and R. N. Zare, “Current-monitoring method for measuring the electroosmotic flow rate in capillary zone electrophoresis,” *Anal.Chem.Analytical Chemistry*, vol. 60, no. 17, pp. 1837–1838, 1988. ID: 4666068784.

- 
- [31] Z. Almutairi, T. Glawdel, C. Ren, and D. Johnson, "A y-channel design for improving zeta potential and surface conductivity measurements using the current monitoring method," *Microfluidics and Nanofluidics*, vol. 6, no. 2, pp. 241–251, 2009. ID: 439054233.
- [32] S. Arulanandam and D. Li, "Determining zeta potential and surface conductance by monitoring the current in electro-osmotic flow," *Journal of colloid and interface science*, vol. 225, no. 2, pp. 421–428, 2000. ID: 359723112.
- [33] J. Anderson and W. K. Idol, "Electroosmosis through pores with nonuniformly charged walls," *Chem.Eng.Comm.Chemical Engineering Communications*, vol. 38, no. 3, pp. 93–106, 1985. ID: 4658840330.
- [34] D. E. Yates, S. Levine, and T. W. Healy, "Site-binding model of the electrical double layer at the oxide/water interface," *J. Chem. Soc., Faraday Trans. 1*, vol. 70, pp. 1807–1818, 1974.
- [35] C. DY, H. TW, S. T, and U. S, "Electrical double layer interactions between dissimilar oxide surfaces with charge regulation and stern-grahame layers.," *Journal of colloid and interface science*, vol. 296, no. 1, pp. 150–8, 2006. ID: 110481039.
- [36] A. Revil, P. A. Pezard, and P. W. J. Glover, "Streaming potential in porous media, 1, theory of the zeta potential," *Journal of geophysical research*, vol. 104, no. B9, p. 20, 1999. ID: 107055634.
- [37] B. CL, P. MV, and D. JA, "Modeling the zeta potential of silica capillaries in relation to the background electrolyte composition.," *Electrophoresis*, vol. 24, no. 10, pp. 1587–95, 2003. ID: 110817576.
- [38] R. HUNTER, "The dependence of electrokinetic potential on concentration of electrolyte," *Journal of Colloid and Interface Science Journal of Colloid and Interface Science*, vol. 37, no. 3, pp. 564–580, 1971. ID: 4662601728.
- [39] D. JE, G. J, E. JA, and R. M, "Dependence of electroosmotic flow in capillary electrophoresis on group i and ii metal ions.," *Journal of chromatography.B, Biomedical applications*, vol. 657, no. 2, pp. 401–7, 1994. ID: 120679432.
- [40] L. Bousse and S. Mostarshed, "The zeta potential of silicon nitride thin films," *Journal of Electroanalytical Chemistry Journal of Electroanalytical Chemistry*, vol. 302, no. 1-2, pp. 269–274, 1991. ID: 4651479963.

- 
- [41] H. Li and P. D. Bruyn, “Electrokinetic and adsorption studies on quartz,” *Surface Science*, vol. 5, no. 2, pp. 203 – 220, 1966.
- [42] A. M. Gaudin, D. W. Fuerstenau, and O. R. O. not identified, “Streaming potential studies. quartz flotation with cationic collectors,” *Mining Eng.*, vol. Vol: 7, pp. 958–62, 1955. ID: 4433737888.
- [43] J. Caslavská and W. Thormann, “Electrophoretic separations in pmma capillaries with uniform and discontinuous buffers,” *Journal of Microcolumn Separations*, vol. 13, pp. 69–83, 2001. ID: 206356834.
- [44] E. Rodier and J. Dodds, “Streaming current measuring for determining the zeta potential of granular particles,” *Particle and particle systems characterization : measurement and description of particle properties and behavior in powders and other disperse systems.*, vol. 12, no. 4, p. 198, 1995. ID: 90491818.
- [45] C. Schwer and E. Kenndler, “Electrophoresis in fused-silica capillaries: the influence of organic solvents on the electroosmotic velocity and the .zeta. potential,” *Anal.Chem.Analytical Chemistry*, vol. 63, no. 17, pp. 1801–1807, 1991. ID: 4666072907.